Evaluation of Molecular Photophysical and Photochemical Properties Using Linear Response Time-Dependent Density Functional Theory with Classical Embedding: Successes and Challenges

WanZhen Liang, 1, a) Zheng Pei, 1 Yuezhi Mao, 2, b) and Yihan Shao 3, c)

¹⁾State Key Laboratory of Physical Chemistry of Solid Surfaces, Collaborative Innovation Center of Chemistry for Energy Materials, Fujian Provincial Key Laboratory of Theoretical and Computational Chemistry, and Department of Chemistry, College of Chemistry and Chemical Engineering, Xiamen University, Xiamen 361005, P. R. China.

(Dated: 10 May 2022)

Time-dependent density functional theory (TDDFT) based approaches have been developed in recent years to model the excited-state properties and transition processes of the molecules in gas-phase and in a condensed medium such as in solution and protein microenvironment or near semiconductor and metal surfaces. In the latter case, usually classical embedding models have been adopted to account for the molecular environmental effects, leading to the multi-scale approaches of TDDFT/PCM and TDDFT/MM, where a molecular system of interest is designated as the quantum mechanical region and treated with TDDFT, while the environment is usually described using either a polarizable continuum model (PCM) or a (non-polarizable or polarizable) molecular mechanics (MM) force fields. In this perspective, we briefly review these TDDFT-related multi-scale models, with a specific emphasis on the implementation of analytical energy derivatives such as the energy gradient and Hessian, the nonadiabatic coupling, the spin-orbit coupling and the transition dipole moment as well as their nuclear derivatives for various radiative and radiativeless transition processes among electronic states. Three variations of the TDDFT method, the Tamm-Dancoff approximation (TDA) to TDDFT, spin-flip DFT, and spin-adiabatic TDDFT, are discussed. Moreover, using a model system (pyridine-Ag₂₀ complex), we emphasize that caution is needed to properly account for system-environment interactions within the TDDFT/MM models. Specifically, one should appropriately damp the electrostatic embedding potential from MM atoms and carefully tune the van der Waals interaction potential between the system and the environment. We also highlight the lack of proper treatment of charge transfer between the QM and MM regions as well as the need for accelerated TDDFT modelings and interpretability, which call for new method developments.

Keywords: TDDFT; Analytic derivatives; Molecule in complex environment, QM-MM interactions

I. INTRODUCTION

To study the systems at the atomic and molecular levels, one has to follow the principles of quantum mechanics (QM). Even though the first-principles electronic structure theory and the quantum dynamics methods have achieved great success in describing the ground state of molecular systems, computing excited electronic state still faces many challenges because it implies not only to find higher-energy solution of the electronic Schrödinger equation, but also to solve many challenging conceptual and technical problems such as the electron-nuclear coupling, the state mixing of the same spin and different spin multiplicities, or the entangled optical and dark processes, which usually require one to abandon the approximations like the adiabatic Born-Oppenheimer(BO) and to calculate the accurate structure properties such as potential energy surfaces, nuclear forces, harmonic and non-harmonic vibrational frequencies, nonadiabatic couplings (NAC), and spin-orbit couplings (SOC). Furthermore, most of the pho-

a)Electronic mail: liangwz@xmu.edu.cn b)Electronic mail: yuezhi.mao@stanford.edu tophysical and photochemical processes of technological and biological interest take place in the condensed phase or in presence of an environment surrounding the molecular system such as solvents, protein scaffolds, and near semiconductor or metal surfaces. In this case, one has to account for the system-environment interaction for properly describing these processes.²

For composite systems like solute-solvent systems, fluorescent proteins, and even nanostructures which integrate molecules or semiconductors with metal nanoparticles (MNPs), a small region of the system plays a predominant role in the excited-state properties and processes of the whole system. Thus, the total system can usually be partitioned into an active region ranging from a single molecule to a molecular aggregate and an embedding environment. The former is mainly responsible for the observed process or property and the latter does not take a direct part in the process but acts as a perturbation affecting the electronic structure and the dynamics of the core active system. The active region is then treated by a high-level QM method, whereas the rest is described by a lower-level approach such as molecular mechanical force fields and continuum models. The integration of QM methods with classical descriptions within multiscale models provides a natural way to focus the computation on a

²⁾Department of Chemistry, Stanford University, Stanford, CA 94305, United States.

³⁾Department of Chemistry and Biochemistry, University of Oklahoma, Norman, OK 73019, United States.

c)Electronic mail: yihan.shao@ou.edu

small area in a larger environment without significantly increasing the computational cost.³ Currently, scientists have developed a family of multiscale theoretical models such as QM/MM (the hybrid QM and molecular mechanics (MM) approach),^{4,5} QM/PCM (the hybrid QM and the polarizable continuum model),^{6,7} QM/MM/PCM,⁸ and QM/EM (the hybrid QM and electromagnetic mechanics or electrodynamics method).^{9–12}

The QM methods for describing the molecular electronic systems can be divided into three categories: semi-empirical quantum chemistry methods, ab initio wavefunction-based methods, and density functional theory (DFT) methods. ¹³ The post-Hartree-Fock(HF) methods have been very successful in describing the ground and excited-state electronic states of small molecules, especially when the molecules are near the equilibrium configuration. The semi-empirical methods are much faster than the ab initio ones. However, they require a couple of atom-specified parameters and are thus only suitable for parameterized systems. For a medium and even large sized molecular system, the most widely used method is DFT. The last two decades have witnessed an explosion of DFT-based calculations in the field of computational chemistry. 14–16 The modeling of ground state processes such as chemical, ¹⁷ surface, ¹⁸ and enzyme reactions, ¹⁹ are mostly carried out using Kohn-Sham DFT (KS-DFT)^{20,21} calculations. Meanwhile, excited-state processes (such as UVvis absorption, ^{22–25} fluorescence, ^{26,27} phosphorescence, ^{28–30} chemiluminescence, ³¹ bioluminescence, ^{32–34} and energy transfer processes in natural and artificial photosynthetic systems, organic and dye-sensitized solar cells, 35-40 etc.) have been modeled extensively using time-dependent DFT (TDDFT), 41,42 which is the excited-state counterpart of the KS-DFT.

The vast popularity of KS-DFT and TDDFT calculations arises from three factors. The first is their costeffectiveness. They are simply orders of magnitudes cheaper than highly reliable quantum chemistry methods such as coupled-cluster methods, ^{43,44} equation-of-motion coupled-cluster methods, ^{45–49} and multi-configurational and multireference wavefunction methods. 50-52 Moreover, the highorder energy derivatives, transition couplings, or molecular properties from DFT and TDDFT are relatively simple to be implemented and cost-efficient, which are essential for studying the rich chemical and physical events we are interested in, e.g., the evaluation of spectroscopic intensities and rates and quantum yields of excited-state processes. The second is their reasonable accuracy, if a suitable exchange-correlation (XC) functional is employed for the particular problem at hand. For example, a valence electronic excitation might be best described with a conventional hybrid functional (such as B3LYP and PBE0), whereas a charge-transfer or Rydberg excitation necessitates the use of range-separated hybrid functionals. 53,54 Besides the above two factors, the DFT/TDDFT methods have also been implemented in many efficient and user-friendly commercial or noncommercial software packages that were developed and made accessible to a wide community of researchers. This wide availability of DFT/TDDFT methods in modern computational chemistry programs, combined with versatile and user-friendly visualization tools, makes them accessible to researchers with no sophisticated background in theoretical chemistry.

Two versions of TDDFT implementation have been familiar to the quantum chemistry community. One is to numerically solve the time-dependent Kohn-Sham equations directly in real-time domain (RT-TDDFT).⁵⁵ RT-TDDFT approach has been implemented in the real space, in plane wave bases and in atomic orbital basis sets, and has been used to calculate the linear and nonlinear spectra, describe the photochemistry by combining the Ehrenfest or surface hopping nuclear dynamics, etc. Many review articles have summarized the recent progress of RT-TDDFT approaches (e.g. Refs. 56-60 and references therein). The other is the implementation of TDDFT at the linear response level (LR-TDDFT), 61-66 which looks like the standard implementation of LR-TDHF already available in most quantum chemistry codes. A set of static Casida's equations was derived and solved to obtain the molecular excitation energies and transition vectors, as well as the oscillator strengths. Within the framework of LR-TDDFT, nuclear gradient^{67–69} and Hessian^{70,71} of excited-state energies, and the nonadiabatic coupling between electronic states 72-74 have all been implemented. Consequently, this LR-TDDFT scheme has become the most widely-used one to extract the energies of low-lying excited states, optimize excited-state geometries, calculate Stokes shifts, and explore the excited-state potential energy surfaces. Here, we only focus on reviewing approaches based on LR-TDDFT, with a specific emphasis on their applications to the calculation of electronic structure quantities required by describing molecular excited-state properties and processes.

Most earlier TDDFT calculations were focused on gasphase excited states. But as mentioned earlier, there has been an ever-growing interest to extend these calculations to composite systems for the modeling of excited-state processes of a single or a few molecules embedded in a condensedphase medium such as solvents, 75–77 macromolecules, 78–80 and metal nanoparticles. ^{10,81–84} For these system-environment complexes, multiscale modeling approaches have been proposed with different level of theories for the different regions. There are generally two categories of embedding methods for TDDFT calculations within the environment: density embedding and classical embedding. Within the category of density-embedding schemes, recent efforts include the projection-based embedding theory, 85,86 frozen-density embedding,⁸⁷ polarized many-body expansion scheme,⁸⁸ etc. When the excited states of molecular aggregates are considered, the subsystem TDDFT methods have shown accuracy and efficiency for large systems⁸⁹ and inter-region charge-transfer excitations. 90,91 On the other hand, the hybrid OM/MM method has been more commonly used in TDDFT calculations with the aforementioned classical embedding, such as QM/MM, QM/PCM, QM/MM/PCM, and QM/EM. In the following, we mainly focus on TDDFT calculations with a classical embedding description of the environment using either PCM^{6,7} or polarizable MM force fields (MMpol).⁹²

While tremendous progress has been made in TDDFT/PCM and TDDFT/MM methodologies, the ap-

plication of these methods to model excited-state properties and processes in a condensed-phase medium still faces three great challenges (in addition to the choice of suitable DFT XC functionals):

- System-environment interactions. For each system-environment complex, there lacks a standard protocol for tuning the QM/MM electrostatic and van der Waals interactions between the system and its environment, which is critical to avoid over-polarization and geometry distortions. Also missing are approaches for describing full charge transfer excitations that move system electrons into the environment or partial charge transfer excitations where the participating system orbitals extend into the environment.
- Computational cost. Standard single-point TDDFT excitation energy calculations and geometry optimizations are currently limited to systems with up to a couple of hundred atoms. To theoretically study a variety of molecular excited-state properties and processes, one has to calculate the derivatives of excitation energies with respect to perturbation parameters such as the nuclear coordinates and external fields, the NACs, the nuclear derivatives of the transition dipole or SOC matrix element, etc. These quantities require even much higher computational cost than the excitation energy calculation. Another bottleneck in TDDFT/MMpol calculations arises from the need to solve for polarizable charges or dipoles, which can become rather expensive with a large polarizable MM region. 93,94
- *Interpretability.* While numerous TDDFT calculations are routinely performed on new dye molecules, bioluminescence probes, etc., few analysis tools beyond electron (difference and transition) densities, atomic partial charges, and excited-state and transition dipole moments are available for helping directly interpret the observed photochemical properties. New analysis procedures and design principles only started to emerge recently for predicting the substituent, solvent, and macromolecular effects on the measured spectra and quantum yield. 96–100

This perspective is organized as follows. In Section II, we briefly introduce a variety of electronic structure quantities required by the evaluation of molecular properties, which are closely related to the calculations of the derivatives of the energy or wavefunction with respect to the nuclear coordinates or other perturbation parameters. The current development of hybrid TDDFT with MM and PCM are summarized in Section III, which is followed by a discussion on the choice of TDDFT methods in Section IV. We then elaborate in Section V on the three challenges listed above for the TDDFT modeling of excited-state processes in complex environments. A summary statement will be given in Section VI.

II. A VARIETY OF ELECTRONIC STRUCTURE QUANTITIES FOR EVALUATION OF MOLECULAR PHOTOPHYSICAL AND PHOTOCHEMICAL PROPERTIES

A. Quantities for Describing Properties of a Specific Electronic Excited State

Molecular properties characterize molecules and their behaviors, and they represent the link between experimental observable quantities and theoretical calculations. There are a wide variety of molecular properties, which are related to numerous physical phenomena. At first we address a variety of properties of molecules at a given electronic state which are related with the calculations of energy derivatives with respect to the perturbation parameters. 101,102 For example, the forces and the force constants are given as the first and second derivatives of the molecular energy with respect to the nuclear coordinates, respectively, ^{67,103} and the infrared intensities can be computed as the cross second derivatives of the molecular energy with respect to the components of a static electric field and nuclear coordinates. 104–106 As such, formulating energy derivatives with respect to the external perturbation variables yields a wealth of time-independent molecular properties.

1. The Excited-State Energy Gradient and Hessian within TDDFT

The energy gradient and hessian with respect to nuclear coordinates have been widely used to explore molecular potential energy surfaces and to calculate vibrational spectra and thermochemical parameters. For a given molecular geometry, the energy of the I-th excited state can be expressed as the sum of the ground-state energy and the excitation energy

$$E_I = E_g + \omega_I, \tag{1}$$

where E_g is the ground-state energy and ω_I is the TDDFT excitation energy of the *I*-th excited state. Then, the energy derivatives of a given excited state *I* can be evaluated as the sum of the ground-state energy derivatives and the derivatives of the corresponding TDDFT excitation energy.

In the framework of LR-TDDFT, the excitation energy is defined as the pole of the LR function to an external perturbation. The excitation energies and the corresponding transition vectors can be obtained from an usual non-Hermitian eigenvalue equation 42

$$\begin{pmatrix} \mathbf{A} & \mathbf{B} \\ \mathbf{B}^{\dagger} & \mathbf{A}^{\dagger} \end{pmatrix} \begin{pmatrix} \mathbf{X} \\ \mathbf{Y} \end{pmatrix} = \boldsymbol{\omega} \begin{pmatrix} 1 & 0 \\ 0 & -1 \end{pmatrix} \begin{pmatrix} \mathbf{X} \\ \mathbf{Y} \end{pmatrix}. \tag{2}$$

The matrix representations of A and B in molecular orbital (MO) basis are written as

$$A_{ia\sigma,jb\sigma'} = \delta_{ab}\delta_{ij}\delta_{\sigma\sigma'}(\varepsilon_{a\sigma} - \varepsilon_{i\sigma'}) + \frac{\partial F_{ia\sigma}}{\partial P_{ib\sigma'}}, \quad (3)$$

$$B_{ai\sigma,bj\sigma'} = \frac{\partial F_{ai\sigma}}{\partial P_{ib\sigma'}}. (4)$$

Here, $\varepsilon_{p\sigma}$ is the p-th σ ($\sigma = \alpha$ or β) spin Kohn-Sham MO energy. The indices i, j, k, \ldots ; a, b, c, \ldots ; and p, q, r, \ldots denote occupied, virtual, and generic MOs, respectively. The transition vectors $|\mathbf{X}\rangle$ and $|\mathbf{Y}\rangle$ are defined on the same Hilbert spaces of $\operatorname{occ} \otimes \operatorname{vir}$, which satisfy the following biorthonormal condition

$$\langle \mathbf{X}_I, \mathbf{Y}_I | \mathbf{X}_J, -\mathbf{Y}_J \rangle = \delta_{IJ}. \tag{5}$$

After these transition vectors are solved, the excitation energy of the *I*-th TDDFT excited state can be expressed as

$$\omega_{I} = \frac{1}{2} (\mathbf{X}_{I} + \mathbf{Y}_{I})^{\dagger} \cdot (\mathbf{A} + \mathbf{B}) \cdot (\mathbf{X}_{I} + \mathbf{Y}_{I})$$
$$+ \frac{1}{2} (\mathbf{X}_{I} - \mathbf{Y}_{I})^{\dagger} \cdot (\mathbf{A} - \mathbf{B}) \cdot (\mathbf{X}_{I} - \mathbf{Y}_{I}). \tag{6}$$

Direct differentiation of ω_I in Eq. (6) with respect to the nuclear coordinates (**R**) requires one to calculate first-order nuclear derivatives of molecular orbital coefficients (**C**) and transition vectors (**X** and **Y**). In order to avoid these calculations, one would define an auxiliary energy functional as⁶⁸

$$\mathcal{L}_{e}[\mathbf{X}, \boldsymbol{\omega}_{I}, \mathbf{C}, \mathbf{Z}, \mathbf{W}] = E_{g} + \boldsymbol{\omega}_{I} - \lambda_{I} (\operatorname{Tr}(\mathbf{X}_{I}^{2} - \mathbf{Y}_{I}^{2}) - 1) + \sum_{ai\sigma} Z_{ai\sigma} F_{ai\sigma} + \sum_{pq\sigma} W_{pq\sigma} (S_{qp\sigma} - \delta_{pq}).$$
(7)

With the construction of the Lagrangian \mathcal{L}_e , one has

$$\frac{dE_I}{dR_i} = \frac{\partial \mathcal{L}_e}{\partial R_i},\tag{8}$$

since \mathcal{L}_e is stationary with respect to all the variational parameters, including \mathbf{C} , \mathbf{X} , and \mathbf{Y} . The Lagrange multipliers \mathbf{Z} and \mathbf{W} are determined by the condition

$$\frac{\partial \mathcal{L}_e}{\partial C_{\mu\nu\sigma}} = 0, \tag{9}$$

and the equation derived thereof is called the *z*-vector equation. 107 Once the energy gradient of an excited state is formulated, one can straightforwardly differentiate the energy gradient to derive the excited-state Hessian. The calculation of excited-state Hessian requires one to calculate the first-order nuclear derivatives of molecular orbital coefficients (\mathbf{C}^R) and transition vectors (\mathbf{X}^R and \mathbf{Y}^R) explicitly, which can be obtained by solving the coupled perturbed self-consistent field (CPSCF) equations 103 and CP-TDDFT equations 71 , respectively. A detailed formulation of the energy Hessian of TDDFT excited states can be found in Refs. 70 (with TDA) and 71 (full TDDFT). The reader is referred to Refs. 69–71,108–116 for additional details.

2. Electric Dipole Moments, Polarizabilities, and Infrared/Raman Intensities

The molecular dipole moment and polarizability of a given electronic state are defined as

$$\mu_x = -\frac{\partial E}{\partial F_x},\tag{10}$$

$$\alpha_{xy} = \frac{\partial \mu_x}{\partial F_y} = -\frac{\partial^2 E}{\partial F_x \partial F_y},\tag{11}$$

where F_x/F_y are the x/y components of the perturbing electric field. The expectation value of the electric dipole moment of a specific electronic state I is usually calculated as

$$\bar{\mu}_{x}^{I} = \langle \Psi_{I} | \hat{\mu}_{x} | \Psi_{I} \rangle = \text{Tr}(\mathbf{P}_{I} \mu_{x}). \tag{12}$$

For the *I*-th excited state, its one-electron reduced density matrix, \mathbf{P}_I , is composed of 70,71,116,117

$$\mathbf{P}_I = \mathbf{P}_0 + \Delta \mathbf{P}_I + \mathbf{Z}_I. \tag{13}$$

Here \mathbf{P}_0 is the reduced one-electron density matrix of the ground state; $\Delta \mathbf{P}_I$ is the *unrelaxed* difference density matrix: $\Delta \mathbf{P}_I = \frac{1}{2} \mathbf{C}_{\mathrm{V}} (\mathbf{X}_I + \mathbf{Y}_I) (\mathbf{X}_I + \mathbf{Y}_I)^\dagger \mathbf{C}_{\mathrm{V}}^\dagger + \frac{1}{2} \mathbf{C}_{\mathrm{V}} (\mathbf{X}_I - \mathbf{Y}_I) (\mathbf{X}_I - \mathbf{Y}_I)^\dagger \mathbf{C}_{\mathrm{V}}^\dagger - \frac{1}{2} \mathbf{C}_{\mathrm{O}} (\mathbf{X}_I + \mathbf{Y}_I)^\dagger (\mathbf{X}_I + \mathbf{Y}_I) \mathbf{C}_{\mathrm{O}}^\dagger - \frac{1}{2} \mathbf{C}_{\mathrm{O}} (\mathbf{X}_I - \mathbf{Y}_I)^\dagger (\mathbf{X}_I - \mathbf{Y}_I) \mathbf{C}_{\mathrm{O}}^\dagger$, where \mathbf{C}_{O} and \mathbf{C}_{V} are the occupied and virtual MO coefficient matrices, respectively; Z_I corresponds to the *z*-vector, denoting the *relaxed* part of the excited-state density matrix.

Moreover, the *I*-th electronic state's polarizability tensor can be calculated as,

$$\bar{\alpha}_{xy}^{I} = \text{Tr}(\mathbf{P}_{I}^{F_{y}}\mu_{x}), \tag{14}$$

where $\mathbf{P}_{I}^{F_{y}}$ denotes the derivative of the one-electron density matrix of a given electronic excited state with respect to the y component of an external field. This expression indicates that it is much easier and faster to calculate the polarizability than the nuclear Hessian because the former is merely related to the energy derivatives with respect to external electric fields so that the explicit derivatives of atomic orbitals in one- and two-electron integrals with respect to nuclear coordinates are not required.

One may be further interested in the nuclear derivatives of the above two quantities (μ and $\bar{\alpha}$) since they are closely related to the calculations of infrared (IR) and Raman intensities, respectively. In the harmonic approximation, the transition electric dipole moment, $\langle \mu_{fi}^I \rangle$, and the polarizability, $\langle \alpha_{fi}^I \rangle$, between the initial and final vibronic states, which enter the expressions of IR absorption and Raman scattering intensities, can be expanded in a power series of the molecular normal coordinates O as

$$\langle \mu_{fi}^I \rangle = \bar{\mu}^I(0) \langle \Lambda_{If} | \Lambda_{Ii} \rangle + \sum_k \left(\frac{\partial \bar{\mu}^I}{\partial Q_k} \right)_0 \langle \Lambda_{If} | Q_k | \Lambda_{Ii} \rangle + \cdots,$$
(15)

$$\langle \alpha_{fi}^I \rangle = \bar{\alpha}^I(0) \langle \Lambda_{If} | \Lambda_{Ii} \rangle + \sum_k \left(\frac{\partial \bar{\alpha}^I}{\partial Q_k} \right)_0 \langle \Lambda_{If} | Q_k | \Lambda_{Ii} \rangle + \cdots.$$
(16)

Under the dipole approximation, the IR intensity corresponding to the transition from the *i*-th vibrational state associated with the electronic state *I* to the *f*-th vibrational state within the same electronic state is proportional to $\left(\frac{\partial \bar{\mu}^I}{\partial Q_k}\right)_0^2$, and the Raman intensity is closely related to the calculation of nuclear derivatives of molecular polarizability. Here we assume that the pure-spin BO (psBO) wavefunctions of initial and final vibronic states can be written as products of an

electronic wavefunction Ψ and a vibrational wavefunction Λ like ${}^{\sigma}\Phi_n(q,Q) = {}^{\sigma}\Psi_N(q,Q)\Lambda_{Nn}(Q)$, with normal coordinates $Q_k = \sum_{i=1}^{3N} l_{ik}q_i$. The q_i 's denote the mass-weighted Cartesian coordinates and the transformation coefficients l_{ik} are chosen such that the potential energy does not depend on cross products.

B. Quantities for Describing Transitions between Electronic States

Transition couplings between different electronic states play central roles in many physical and chemical processes. To characterize a photophysical process such as optical absorption and radiative emission (fluorescence and phosphorescence) or radiativeless transition such as internal conversion (IC), intersystem crossing (ISC), and decay through conical intersection (CI), one usually has to account for simultaneous changes in the vibrational and electronic states. Within the perturbation theory framework, one will need to combine the electronic structure theories and the quantum dynamics methods. The former is adopted to obtain the electronic structure parameters and the latter is used to describe the nuclear dynamics.

According to the Fermi's golden rule, 122 the transition rate (k) from the initial state i to a dense manifold of final states f can be defined as

$$k_{i} = \frac{2\pi}{\hbar} \sum_{f} \left\langle \Phi_{f} \middle| \hat{H}' \middle| \Phi_{i} \right\rangle^{2} \delta \left(\hbar \omega - (E_{f} - E_{i}) \right), \tag{17}$$

where Φ_i and Φ_f are the wavefunctions of the initial and final vibronic states, respectively, ω is the frequency of the external radiation. $\hat{H}' = \hat{H} - \hat{H}^{el}$ (the electronic Hamiltonian) denotes the perturbation Hamiltonian and can be written as

$$\hat{H}' = -\vec{\mu} \cdot \vec{f} + \hat{T}_{N} + \hat{H}_{SO}, \tag{18}$$

where the first, second, and third operators correspond to the matter-field interaction, the nuclear kinetic energy, and spin-orbit interaction, respectively. The radiative transition like electronic absorption or emission is usually governed by the matrix element of $\langle \Phi_f | \hat{\mu} | \Phi_i \rangle$ while the nonradiative processes like IC and ISC or reversed ISC (RISC) are determined by the matrix elements of the latter two operators, respectively. For example, if we restrict ourselves up to second-order terms, the coupling matrix element of an ISC process can be

expressed as

$$H'_{fi} = \langle {}^{3}\Phi_{f} | \hat{H}_{SO} | {}^{1}\Phi_{i} \rangle + \sum_{m \neq i} [\langle {}^{3}\Phi_{f} | \hat{H}_{SO} | {}^{1}\Phi_{m} \rangle \langle {}^{1}\Phi_{m} | \hat{T}_{N} | {}^{1}\Phi_{i} \rangle / (E_{i} - E_{m})] + \sum_{m \neq f} [\langle {}^{3}\Phi_{f} | \hat{T}_{N} | {}^{3}\Phi_{n} \rangle \langle {}^{3}\Phi_{n} | \hat{H}_{SO} | {}^{1}\Phi_{i} \rangle / (E_{f} - E_{n})], = H_{SO}^{FI} |_{Q=0} \langle \Lambda_{Ff}(Q') | \Lambda_{Ii}(Q) \rangle + \sum_{k=1}^{3N-6} \left(\frac{\partial H_{SO}^{FI}}{\partial Q_{k}} |_{Q=0} \langle \Lambda_{Ff}(Q') | Q_{k} | \Lambda_{Ii}(Q) \rangle \right) - \sum_{k=1}^{3N-6} \left[\sum_{M \neq I} \frac{H_{SO}^{FM} d_{MI,1}^{k}}{(E_{I} - E_{M})} + \sum_{N \neq F} \frac{d_{FN,3}^{k} H_{SO}^{NI}}{(E_{F} - E_{N})} \right]_{Q=0} \times \langle \Lambda_{Ff}(Q') | \frac{\partial}{\partial Q_{k}} | \Lambda_{Ii}(Q) \rangle$$

$$(19)$$

Here the summations extend over the complete sets of psBO vibronic states of the given multiplicity and the psBO wavefunctions of the initial and final vibronic states have been written as products of an electronic wavefunction Ψ and a vibrational wavefunction Λ . The relation

$$\langle {}^{\sigma}\Phi_{e} \mid \hat{T}_{N} \mid {}^{\sigma}\Phi_{r} \rangle \sim -\hbar^{2} \sum_{k=1}^{3N-6} \langle {}^{\sigma}\Psi_{E} \mid \nabla_{k} \mid {}^{\sigma}\Psi_{R} \rangle \langle \Lambda_{Ee}(Q') | \nabla_{k}\Lambda_{Rr}(Q) \rangle$$

$$(20)$$

has been applied, and

$$d_{ER,\sigma}^{k} = \langle {}^{\sigma}\Psi_{E} \mid \partial/\partial Q_{k}{}^{\sigma}\Psi_{R} \rangle \tag{21}$$

is defined as the NAC vector between two excited states of the given spin multiplicity σ . The spin-orbit coupling matrix element (SOCME) has been assumed to be normal mode-dependent, and it reads

$$H_{SO}^{FI} = \langle \Psi_F | \hat{H}_{SO} | \Psi_I \rangle = H_{SO}^{FI}(Q=0) + \frac{\partial H_{SO}^{FI}}{\partial Q} |_{Q=0}Q + \cdots,$$
(22)

which thus includes the Franck-Condon (FC) and Herzberg-Teller (HT) contributions. Although Eq. (19) specifically refers to a $S \rightarrow T$ crossing, the corresponding expression for the RISC is readily written down.

The transition dipole moment between pure S_0 and T_1 states is zero. In the case of phosphorescence, one has to resort to perturbation theory by considering the SOC perturbation to give rise to admixtures of states with opposite spin.

It is clear that to quantitatively describe the radiative and radiationless processes such as the molecular vibronic spectra¹²³ and the transition rates within the perturbation theory framework, one has to know the geometric and electronic structure parameters at first. More specifically, the energy gradients of ground and excited states are required to reach the minimum on each potential energy surface. Meanwhile, Hessians of the ground- and excited-state energies are indispensable for acquiring the normal modes for each electronic state, establishing the Duschinsky relation, ¹²⁴ as well as incorporating the FC/HT and HT contributions.

1. Non-Adiabatic Coupling

The nonadiabatic coupling (NAC) is needed as long as the psBO approximation breaks down, which is quite common for radiationless processes such as IC, 125 decay through CI, 126,127 and potentially ISC and RISC. These nonadiabatic transitions are governed by \hat{T}_N mentioned in Eq. (18), and the NAC between two vibronic states could be derived as 128

$$H_{\text{NAC}} = \left\langle \Phi_{m}(q, Q) \middle| -\frac{\hbar^{2}}{2} \sum_{k} \frac{\partial^{2}}{\partial Q_{k}^{2}} \middle| \Phi_{n}(q, Q) \right\rangle$$

$$\sim -\hbar^{2} \sum_{k} d_{mn}^{k} \left\langle \Lambda_{m}(Q) \middle| \frac{\partial \Lambda_{n}(Q)}{\partial Q_{k}} \right\rangle, \tag{23}$$

where \hat{T}_N is split into two momentum operators for electronic and vibrational states, respectively, and

$$d_{mn}^{k} = \left\langle \Psi_{m}(q, Q) \middle| \frac{\partial \Psi_{n}(q, Q)}{\partial Q_{k}} \right\rangle \tag{24}$$

is the derivative coupling (DC). The DC associated with TDDFT excited states can be formulated using the equation-of-motion (EOM) and response theory 72,73,129 or pseudo-wavefunction approach. The DC implementations with different DFT methods are summarized in Table I. In short, it is not necessary to explicitly solve for either orbital responses or amplitude derivatives in the computation of d_{mn}^k ; only one z-vector needs to be solved for instead. One may refer to Ref. 131 for a review about the derivative couplings in TDDFT.

2. Transition Dipole Moment and Its Nuclear Derivatives

For studying radiative transitions, the transition dipole moment μ and frequently its nuclear derivative need to be calculated. Like SOCME in Eq. (22), μ can also be expanded as

$$\begin{split} \langle \Lambda_{Gg} | \mu^{GK} | \Lambda_{Kk} \rangle &= \mu^{GK} (Q=0) \langle \Lambda_{Gg} | \Lambda_{Kk} \rangle + \\ & \sum_{j} \frac{\partial \mu^{GK}}{\partial Q_{j}} |_{Q=0} \langle \Lambda_{Gg} | Q_{j} | \Lambda_{Kk} \rangle + \cdots (25) \end{split}$$

FC approximation just keeps the first term above and takes $\mu^{GK} = \langle \Psi_G | \hat{\mu} | \Psi_K \rangle$ as a constant. The contribution of the second term could also be significant especially when μ^{GK} is small. In these situations, one must invoke the FCHT approximation to take the first two terms into account.

The nuclear derivatives of the transition dipole moments between the ground and excited states can be evaluated as $\mu_{GE}^x = \text{Tr}(\delta \rho^x \mu) + \text{Tr}(\delta \rho \mu^x)$. Here $\delta \rho$ and μ are the transition density matrix and the dipole moment matrix, respectively, in the basis of molecular or atomic orbitals. Observably, μ_{GE}^x is the reference geometry-dependent. The $\delta \rho^x$ has already been evaluated during the analytical calculation of the excited-state Hessian, as showed in Refs. 70 (with TDA) and 71 (full TDDFT). Therefore, the computational time will be saved if one obtains μ_{GE}^x as a byproduct of the calculation of excited-state Hessian.

3. SOC Matrix Element between Different Electronic States and Its Nuclear Derivatives

The SOC operator acts on both the angular and spin components of electronic states, leading to its defining characteristics of mixing the orbital and spin degrees of freedom, thus allowing electronic states of different multiplicities to couple. It plays an essential role in photoinduced phenomena that involve change in the spin multiplicities of electronic states, as it governs the rates of phosphorescence emission ¹³² and ISC/RISC processes. ¹³³ Since TDDFT has been routinely used in studying photoexcited molecular systems, it is desirable to calculate SOC at the TDDFT level of theory.

Given that SOC stems from relativistic Dirac theory, the SOC effects can be taken into account naturally in relativistic TDDFT,¹³⁴ such as the four- and two-component relativistic theories. This type of treatment is rigorous and of high quality, but computational demanding. For molecules in which the SOC is weak and therefore serves as a perturbation, the perturbative approaches are readily applicable. ^{134,135} In this case, the pure-spin states are first obtained from scalar relativistic or non-relativistic LR-TDDFT, ^{136–144} then one could calculate SOC matrix elements among these excited states.

The perturbational treatment is not so accurate as the variational approaches are. But the perturbative SOC approach is less computational demanding and allows one to identify the weights of singlet and triplet characters in a spin-adiabatic state. ¹⁴⁵ Beyond the linear-response regime, the calculation of SOCMEs has also been performed within quadratic-response TDDFT, which can be viewed as implicit sum-over-states compared to perturbation theory. ^{146,147} It is worth noting that Li et al. proposed a novel procedure to calculate SOCMEs from variational relativistic electronic structure theory. ¹⁴⁸

As shown in Eq. (19), the calculation of ISC or RISC rate usually requires one to account for both the HT-type vibronic and the spin-vibronic effects. ^{1,149} The former vibronic effect requires one to know the nuclear derivatives of SOCME, whose analytical implementation is currently under development.

III. ELECTRONIC EXCITED STATES WITHIN TDDFT/PCM AND TDDFT/MM

When a system of interest is embedded into a condensedphase medium, its potential energy surfaces are perturbed, which can potentially cause a substantial change to the molecular properties, spectral profiles, and various transition rates and the corresponding quantum yield.

Due to the formidable computational cost of the realistic complexity, a full-QM modeling of the electronic structure of a system and its environment is usually infeasible. For instance, QM modeling, especially plane-wave density functional theory, has been employed to describe plasmonic metal surfaces and adsorbed reactants in studies of photon-driven catalysis. However, given its steeply increasing cost, routine *ab initio* QM modeling is typically limited to systems (or subsystems) smaller than 2 or 3 nm. This has inspired

TABLE I. Development of Analytical Gradient, Hessian, and Nonadiabatic Coupling (NAC) of Various TDDFT and TDDFT/Classical Em-
bedding Methods.

Method	Energy	Gradient	Hessian	NAC
TDDFT	Ref. 61	Refs. 67,68,108,110,150-154	Refs. 70,71	Refs. 72-74,155-159
SF-DFT	Refs. 160–163	Refs. 164,165		Refs. 166,167
SA-TDDFT	Refs. 130,168	Ref. 168		Refs. 130,169
TDDFT/PCM	Refs. 22,75,170-174	Refs. 69,114,115	Ref. 116	
TDDFT/MM TDDFT/MMpol	Many Refs. 83,92,178–181	Refs. 175 Refs. 111–113,182	Ref. 175	Refs. 176,177

the development of methods for capturing the environment effects via lower-level theories such as classical analytical models (specifically for metal nanoparticles), ^{186–191} implicit solvation models, polarizable or nonpolarizable MM force fields, and coarse-grained models. ¹⁹²

When a chemical system is immersed in liquid solutions, its properties may change significantly, especially in polar solvents. The solvent effects are usually accounted for by a continuum solvent description, such as the family of PCM,^{6,7} or a mixed treatment that integrates different descriptions of the solvent, for example, representing the first solvation shell with explicit solvent molecules while using a continuum model for the bulk. In the PCM method, the electrostatic polarization interaction between solute and solvent is determined via the induced apparent surface charge method, for which one needs to specify a surface that defines the continuum boundary. TDDFT coupled with PCM for excitation energy calculations has become as a general routine in most quantum chemistry software packages. The implementation of analytical gradient 69,114,115 and Hessian 116 of TDDFT/PCM excited states has also been realized by several groups. TDDFT/PCM has been shown to be successful in supporting the analysis of experimental data, providing useful insights for a better understanding of photophysical and photochemical pathways in solution.

The PCM has also been applied to model nanoparticles (NPs), leading to the PCM-NP approach. In the quasi-static limit, the NP experiences an electrostatic potential at a given frequency, which induces polarization charges on the nanoparticle surface. The QM/PCM-NP approach, which explicitly includes mutual polarization effects between the molecule and NP, has been applied to calculate the absorption factor as well as the radiative and nonradiative decay rates.³

The all-atom polarizable molecular mechanical models have emerged in the last decades. Through introducing induced charges and/or dipoles at each atom site of MM region, these MMpol models can efficiently capture the electronic motion in solvents, proteins, and large MNPs (> 10 nm). 193,194 Among the MMpol models for MNPs, of particular interest to us is the discrete interaction model (DIM)83,195,196 and its coordination-dependent variant (cd-DIM), with the induced charges and dipoles representing polarization effects. Several similar all-atom MMpol models have also been developed such as the point-dipole interaction model 197,198 (including its combination with either electronegativity equalization 199 or charge-transfer 200), charge-

dipole interaction model, ^{201,202} and atomic dipole approximation model. ¹⁹⁴ Using a polarizable force field in QM/MM calculations is advantageous in light of the fact that the electronic polarization of the MM region can be described, especially on the occasion when electronic excitation is involved in the QM region.

Comparing with the QM/PCM methods, QM/MM or QM/MMpol approaches, which allow us to incorporate the explicit atomic or molecular details of surrounding molecules, can be applied to more complex environments. There are three embedding schemes for QM/MM, namely, mechanical,²⁰³ electrostatic, and polarizable.²⁰⁴ It is essential to combine TDDFT with MM to explore the molecular excited-state structures and dynamical properties in complex condensedphase systems. Table I summarizes the current status of TDDFT-related approaches. Currently the analytic nuclear gradients of TDDFT/MM and TDDFT/MMpol excited states are made available by a few groups. The implementation of analytic second-order energy derivatives¹⁷⁵ for TDDFT/MM with a non-polariable force field has also been realized. The newly proposed hybrid methods, TDDFT/DIM (for metal nanoparticles)83,178 and TDDFT/FQFD (for solvents), 181 have only been made available for excitation energy calculations. Note that within the hybrid schemes, NAC calculations have only been carried out using non-polarizable AMOEBA, 176,177 and the incorporation of the environment effect in this model needs to be reviewed carefully.

IV. CHOICE OF TDDFT MODELS

In the TDDFT modeling of electronic transitions, one can choose among several variations of TDDFT methodology for the problem in hand.

A. TDA versus Full-TDDFT

Tamm–Dancoff approximation (TDA) amounts to the negligence of the Casida **B** matrix in the TDDFT working equations. As a result, all **Y** amplitudes become zero. Using perturbation theory, it is easy to show that TDA excitation energies would always be larger than corresponding TDDFT values, with the leading difference being second-order: $\omega_m^{\text{TDA}} - \omega_m^{\text{TDDFT}} \approx \sum_n \left| \mathbf{X}_m^{\text{TDA}} \cdot \mathbf{B} \cdot \mathbf{X}_n^{\text{TDA}} \right|^2 / (\omega_m^{\text{TDA}} + \omega_n^{\text{TDA}})$. In general, **B** matrix elements are relatively small, so TDA pro-

duces results that closely resemble TDDFT values. When using pure functionals (such as BLYP and PBE) or conventional hybrid functionals (such as B3LYP and PBE0), however, full TDDFT tends to systematically underestimate the energy of excited states with a small charge-transfer or Rydberg character. In those cases, as shown in a recent TDDFT benchmarking study,²⁰⁵ TDA can produce slightly more accurate excitation energies than full TDDFT as shown in Fig. 1. On the other hand, for range-separated hybrid functionals, full TDDFT can produce more accurate results (compared to CC2 values). Full TDDFT usually encounters problems with triplet states, because the DFT ground state is used as the reference, which in many cases even leads to triplet instabilities. The TDA can be used to circumvent the triplet instabilities. Furthermore, TDDFT obeys the Thomas-Reiche-Kuhn sum rule of the oscillator strengths, ²⁰⁶ therefore yields more precise results for the oscillator strength and other related physical quantities. The TDA violates the sum rule, which leads to poor results in the calculated oscillator strengths. Interestingly, it is found that the TDA performs better in the calculation of NACs than the full TDDFT, contrary to the conjecture that the TDA might cause the NAC results to deteriorate and violate the sum rule. 207 For the excited-state harmonic vibrational frequencies, however, full TDDFT does not seem to be advantageous since the numerical tests demonstrate that the accuracy of TDDFT with and without TDA are comparable to each other.⁷¹

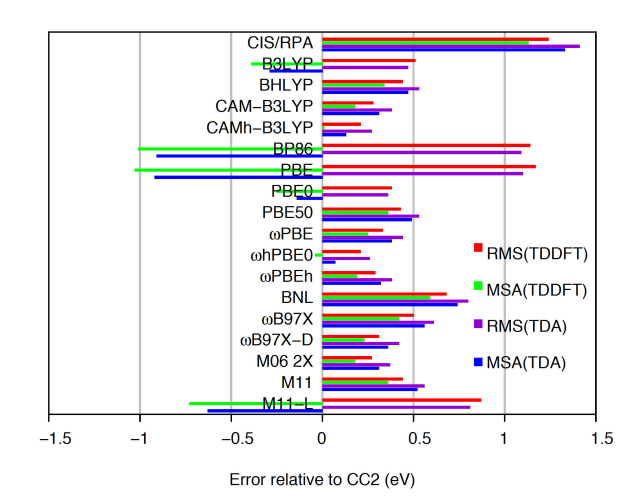


FIG. 1. Root-mean-square (RMS) and mean-signed-average (MSA) differences (in eV) between vertical excitation energies calculated at the TDDFT, TDA, and CC2²⁰⁸ levels using the def2-TZVP²⁰⁹ basis set. Excitation energies of the five lowest excited states of the 11 chromophores are included. Reproduced with permission from J. Chem. Theory Comput. 16, 587 (2019). Copyright 2019 American Chemical Society.

B. Spin-Flip DFT

Spin-flip (SF) DFT, which can be viewed as a special version of TDA, ^{160–162} handles up to four lowest electronic states

of a system with an even number of electrons (two closedshell singlets, an open-shell singlet, and a $m_z = 0$ triplet) on the same footing, thus offering a balanced description for these states. These states are obtained by using a high-spin $(m_z = 1 \text{ triplet})$ reference state and solving the eigenproblem within spin-flip excitations, where an electron is excited from an α occupied molecular orbital to a β virtual orbital. In general, for a system whose ground state has a total spin quantum number S (multiplicity 2S + 1), the reference needs to be in an S+1 state in order to target the lowest-energy states with total spin quantum number S and S+1 via spin-flip excitations. Compared to standard TDA and TDDFT, the spinflip TDA model usually provides more accurate results for diradicals and other systems with multi-reference characters. After the proposition of the original SF-DFT, 160, there have been various improved variations such as the spin-adapted SF-DFT method aiming to eliminate the spin-contamination issue. 163,210,211

When CI appears between the electronic ground state and an excited state, there is an advantage to use SF method to provide a balanced description of the two electronic states. Gordon et al. 180 used the SF-DFT combined with the effective fragment potential (EFP) and illustrated that polar solvents could change the CI geometry dramatically and strongly stabilize its energy. Herbert et al. 166 studied the CI point of the D₀ and D₁ surfaces of the H₃ molecule. They have demonstrated that the SF-CIS and SF-BH&HLYP methods could locate CI points that involve the reference (ground) state correctly, which are problematic for the spin-conserved counterparts of these methods. What's more, equipped with analytic derivative couplings, their method could substantially reduce the cost of locating minimum-energy crossing points. 166

Analytic gradient 164,165 and nonadiabatic coupling 166,167 have been developed for gas-phase SF-DFT calculations, while the analytical Hessian is still under development. As far as we know, there has been no much discussion on SF-DFT/PCM or SF-DFT/MMpol models. Within a linear-response framework, however, a PCM or MMpol modeling of the complex environment is expected to yield no additional contribution to the **A** matrix (due to a transition density in the $\alpha\beta$ block). So, theoretically, it reduces to a "zeroth-order" model, where PCM surface charges or MMpol permanent/induced moments affect the results only by polarizing the KS orbitals.

C. Spin-Adiabatic DFT/TDDFT States

Spin-adiabatic (SA) TDDFT has gained attention only in recent years. 130,168 Compared with the spin-diabatic states, the spin-adiabatic counterparts have shown advantages 130 in Tully's fewest switches surface hopping (FSSH) dynamics 213 to evaluate the rates and branching ratios of ISC processes where spin multiplicity changes. For a system with an even number of electrons, there are 4n+1 spin-diabatic states: the ground state, the lowest n open-shell singlet excited-states and the lowest n triplet excited-states (with $n_s = -1, 0, 1$). They

could be coupled together via the SOC operator:

$$\mathbf{H}^{(0)} + \mathbf{V}^{SO} = \begin{pmatrix} E_{S_0} & 0 & V_{S_0T_1}^{SO} & \cdots & 0 & V_{S_0T_n}^{SO} \\ 0 & E_{S_1} & V_{S_1T_1}^{SO} & \cdots & 0 & V_{S_1T_n}^{SO} \\ V_{T_1S_0}^{T_0} & V_{T_1S_1}^{SO} & E_{T_1} & \cdots & V_{T_1S_n}^{SO} & V_{T_1T_n}^{SO} \\ \cdots & \cdots & \cdots & \cdots & \cdots & \cdots \\ 0 & 0 & V_{S_nT_1}^{SO} & \cdots & E_{S_n} & V_{S_nT_n}^{SO} \\ V_{T_nS_0}^{SO} & V_{T_nS_1}^{SO} & V_{T_nT_1}^{SO} & \cdots & V_{T_nS_n}^{SO} & E_{T_n} \end{pmatrix}$$
 (26)

Note that the couplings between different triplet states could be nonzeros. Formally, all the spin-adiabatic states can be obtained by diagonalizing this $(4n+1) \times (4n+1)$ matrix.

Subotnik and coworkers ^{130,168} implemented an efficient iterative procedure for diagonalizing the above coupling matrix between TDA singlets and triplets, but without including the ground state. Furthermore, they formulated the analytical gradient of the obtained spin-adiabatic TDA states, ¹⁶⁸ and developed the nonadiabatic couplings between the spin-adiabatic TDA states. ¹³⁰ This new and substantial advance is expected to facilitate the study of ISC and allow for a balanced treatment between ISC and IC events.

On the other hand, a future extension of this methodology to include the ground state as well in the coupling (Eq. (26)) would be desirable, which will provide a general framework for, for instance, the study of phosphorescence decay and the construction of spin-adiabatic potential energy surfaces for modeling spin-crossing reactions. Furthermore, in the study of spin-crossing reactions, it was found to be a poor approximation to describe the lowest singlet and triplet states using the same set of molecular orbitals. Therefore, it should be more suitable to have one set of optimized orbitals for the singlet state and another for the triplet state.

V. CHALLENGES WITH TDDFT MODELING OF EXCITED STATES IN THE CONDENSED PHASE

A. Challenges with the Modeling of System-Environment Interactions

To illustrate the challenges in describing several QM–MM interactions of an actual system, a pyridine–Ag₂₀ complex in Fig. 2 is used as a showcase. As shown below, this is a highly challenging system for classical embedding due to the strong interaction between the pyridine molecule and the metal cluster. Our primary focus is on the effect of the metal cluster on electronic excitations within the pyridine molecule. This complex is handled using a QM/DIM model adopted from Jensen et al., ^{83,84,178,215} which combines a DIM description for the Ag₂₀ cluster and a DFT or TDDFT description for pyridine. All calculations are carried out using a preliminary implementation²¹⁶ of the QM/DIM model within the Q-CHEM software package.²¹⁷

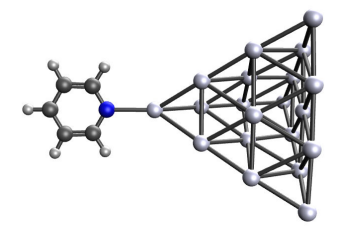


FIG. 2. Scheme of pyridine-silver₂₀ (Py-Ag₂₀) configuration.

1. Charge transfer between QM and MM regions

As indicated by charge populations in Table II, for the electronic ground state of Py–Ag₂₀, there is a charge migration (0.16–0.30 e⁻) from the pyridine molecule to the Ag₂₀ cluster. Energy decomposition analysis (EDA) based on absolutely localized molecular orbitals (ALMO)²¹⁸ for this complex also shows a substantial charge-transfer stabilization (-49.09 kJ/mol) together with a similar amount of polarization energy (-38.83 kJ/mol).

TABLE II. Net charges on the pyridine molecule within Merz-Kollman ESP, 219 ChElPG, 220 and fragment-based Hirshfeld (FBH) 221 charge partitioning schemes and energy decomposition analysis of the ground-state energy of pyridine–silver $_{20}$ complex calculated with the ω B97X-D 222 functional and 6-31G(d) basis set and SRSC ECP.

Q _{Py} (a.u.)			ΔE (kJ/mol)				
QESP	Q ^{ChElPG}	Q ^{FBH}	ΔE_{Frozen}	ΔE_{Pol}	ΔE_{CT}	ΔE_{Total}	
0.30	0.22	0.16	7.68	-38.83	-49.09	-80.23	

Starting from this ground state with partial charge transfer, the lowest 200 excited states from a full-TDDFT calculation are mostly local excitations on the metal cluster, with a few states featuring charge transfer between the molecule and the metal cluster. None of these low-lying states correspond to local excitations on the pyridine molecule. This poses a serious challenge to the modeling of electronic excitations in these complexes, since full or partial charge-transfer excitations are *not* incorporated into the existing hybrid QM/MM approaches such as TDDFT/DIM. Here, state-selective optimization schemes^{223–225} might help capture the local excited states in large systems.

2. Proper damping of QM/MM Electrostatics

To show the effect of the damped QM/MM electrostatics in the QM/DIM modeling of the Py–Ag $_{20}$ complex, several frontier molecular orbital energies are plotted in Fig. 3. The orbital energies for the gas-phase pyridine and the Py–Ag $_{20}$ complex are obtained from DFT/DIM and ALMO-DFT 226 calculations, respectively.

As shown in Fig. 3, all frontier MO energies of the pyridine molecule are shifted down upon its adsorption onto the Ag_{20}

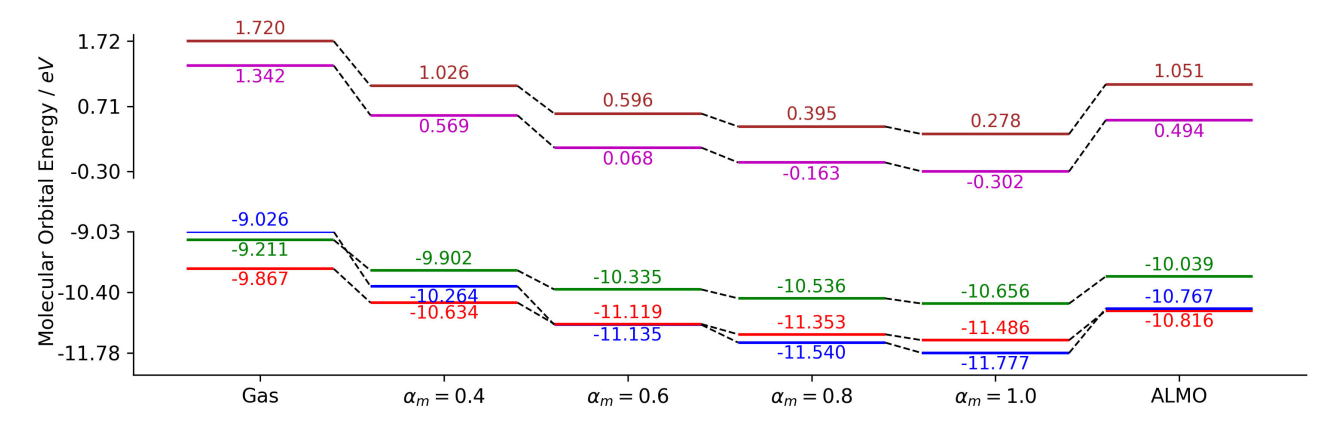


FIG. 3. Frontier orbital energies (3 occupied orbitals and 2 unoccupied orbitals) from DFT calculations of the gas-phase pyridine, DFT/DIM calculations (with Gaussian exponents of 0.4, 0.6, 0.8, and 1.0 a.u.), and ALMO-DFT calculations for the Py–Ag₂₀ complex. All calculations used the ω B97X-D functional, 6-31G(d) basis set, and SRSC ECP.

cluster. The highest occupied molecule orbital (HOMO), which is the only σ -orbital out of the five orbitals, is subjected to the largest decrease in its energy, thus becoming HOMO-1 or HOMO-2 in DFT/DIM and ALMO-DFT calculations. Overall, we find that using a damping factor (α_m) of 0.6 or 0.8 a.u. for the induced dipoles in the DIM model best reproduces the relative energies between these frontier orbitals obtained from the ALMO-DFT reference. The five lowest excitation energies show a similar trend as the frontier orbitals with the increasing damping factor (see Fig. 4). In fact, TDDFT-TDA/DIM calculations with a damping factor α_m of 1.0 au would best reproduce the results of the ALMO-TDDFT-TDA calculations, 97,227 which can be used as the benchmark of the local excited states.

3. Description of QM/MM van der Waals Interactions

The van der Waals (vdW) interactions between the QM and MM regions are crucial for obtaining accurate potential energy profiles. In our implementation of the QM/DIM method, a distance-dependent Lennard-Jones (i.e., 12–6) potential proposed by Jensen and coworkers²¹⁵ is adopted with a small modification. Without the repulsive interaction, the optimized Py–Ag bond would become too short due to a strongly attractive QM/MM electrostatic interaction.

To avoid a system-dependent tuning of QM/MM vdW parameters, as we have done with the ε_0 and ε_1 parameters for the nitrogen atom, one should make the vdW parameters of the QM atoms dependent on the electronic structure (densities, molecular orbitals, or atomic charges) of the QM region. $^{228-230}$ Within the *ab initio* QM/MM framework, one can tap into the Tkatchenko–Scheffler dispersion model, 231 where the C_6 parameter of an atom is computed from its Hirshfeld-weight-based atomic volume in the molecule. This has led to two density-dependent QM/MM vdW models by Cappelli and coworkers 229 and by Mennucci and coworkers, 230 respectively. We expect that these models be further tested and developed before becoming widely

adopted in condensed-phase QM/MM simulations. Alternatively, one can predefine localized molecular orbitals on the MM atoms and interact them with orbitals from the QM region to acquire dispersion and repulsion interactions. This has been implemented in DFT/EFP models.^{232–234}

B. Challenges with the Computational Costs

TDDFT modeling of condensed-phase excited-state processes can become very expensive, especially with a large QM region or a long simulation (1 ps or longer). The first bottleneck of these modelings come from the OM calculation itself, namely the computation of DFT and TDDFT energy gradient/Hessian and state-to-state derivative couplings. It is time-consuming to evaluate many Fock-like or Fockderivative-like matrices, with some of them involving the third and fourth derivatives of the exchange-correlation functional. Two ways can be pursued to accelerate these calculations. First, following Grimme and coworkers, one can approximate the two-electron integrals and transition density, which has led to the simplified TDA scheme for large system.²³⁵⁻²³⁷ Second, one should be able to extrapolate SCF orbitals, TDDFT amplitudes, and z-vectors from previous geometries during a geometry optimization or molecular dynamics simulation. To extrapolate SCF orbitals, the Fock matrix extrapolation scheme from Pulay, Herbert, and others^{238,239} and extended Lagrangian from Niklasson and coworkers^{240,241} can already reduce the SCF cycles. For excited state simulations with TDDFT energies/forces, one should also be able to extrapolate amplitudes and z-vectors in a way similar to the handling of MP2 z-vectors by Steele and Tully.²⁴²

For TDDFT/MMpol with an extended (solvent, protein, or metal-cluster) environment, a second bottleneck comes from the solution of a large number of induced charges/dipoles during each SCF iteration. 3,76,243,244 Several efforts have been devoted to the reduction of this computational cost. 93,94 First, in order to avoid the $\mathcal{O}(N^3)$ complexity associated with directly solving linear equations for induced charges or dipoles,

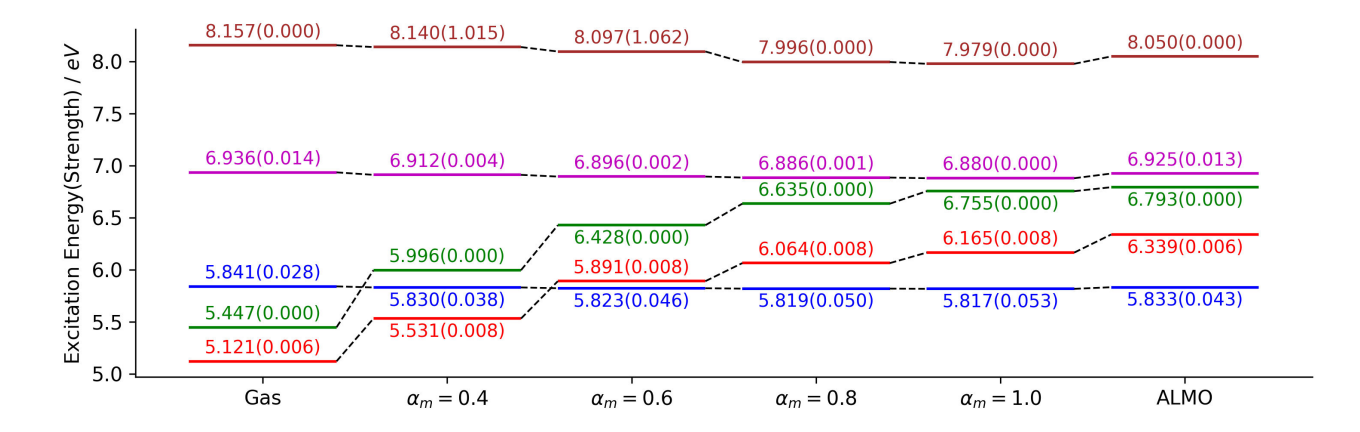


FIG. 4. First five excitation energies from TDDFT-TDA calculations of the gas-phase pyridine, TDDFT-TDA/DIM calculations (with Gaussian exponents of 0.4, 0.6, 0.8, and 1.0 a.u.), and ALMO-TDDFT-TDA calculations for the Py-Ag₂₀ complex. All calculations used the ω B97X-D functional, 6-31G(d) basis, and SRSC ECP.

iterative solvers can be employed, such as Jacobi iterations (JI)^{245–247} and preconditioned conjugate gradient (PCG),²⁴⁸ and the truncated version of JI²⁴⁹ and PCG.^{250,251} For large systems, Nocito and Beran proposed a divide-and-conquer Jacobi iterations (DA-JI) method^{252,253} and also modified an always stable predictor-corrector (ASPC) algorithm.²⁵⁴ Second, one can truncate the mutual polarization among MM atoms such as in the 3-AMOEBA scheme.²⁵⁵ Lastly, the extended Lagrangian method can be employ to remove the need to fully converge MM induced dipoles at each geometry.^{256–258}

C. Challenges with the Interpretability of Computational Results

Fundamentally, we are interested in the effects of various internal and external perturbations on excited-state processes, namely how they shift absorption/emission wavelengths and how they modulate the radiative/nonradiative transition rates and thus change the overall quantum yield. Internally, a system can be "perturbed" by chemical modifications, such as substitutions and combination of different donors/bridges/acceptors. Externally, a system can be placed in different solvents, protein mutants, or metal clusters of various shapes, sizes, and compositions.

TDDFT modeling has proven to be extremely valuable in these studies. In addition to the TDDFT calculations themselves, many efforts have been devoted to the challenging task of analyzing the results of these calculations. Given a computed TDDFT excited state, one can now readily (a) visualize the density change from the ground state, and compute the corresponding charge populations; (b) visualize the canonical orbitals and natural transition orbitals associated with the excitation; and (c) characterize it as being a local excitation, charge-transfer excitation, or a hybrid.

The characterization of the lowest excited states of a system is especially important in many design problems, such as new TADF molecules for which a hybridized local and intramolecular charge-transfer (HLCT) excitation might op-

timally enhance the reverse internal system crossing while retaining a decent fluorescence intensity. The Λ values from Peach and coworkers 259 and charge transfer numbers (CTN) from Plasser and coworkers 260,261 have been widely used for such characterizations.

While the electronic density change upon an excitation is commonly visualized, it was only until recently when one can start to analyze the excitation energy distribution, which can also be of interest. For several example systems, we showed that it is feasible to compute and visualize the LR-TDDFT excitation energy density. ²⁶² It has also provided a way for one to formulate the effective energies of the hole and particle for a charge-transfer excitation.

In the design of new fluorophores/dyes, guiding principles or inexpensive tools are needed to help quickly predict how a chemical modification or environmental change (as mentioned above) might affect the photophysical properties of a fluorophore (dye) molecule. As for many of these fluorophores the HOMO→LUMO transition or other transitions between frontier orbitals play the dominant role, we expect the ALMO-based orbital interaction analysis ^{96,100} to be increasingly used to analyze or predict substituent effects or donor-acceptor interactions. On the other hand, the substitution/mutation effects on the rate of radiative and non-radiative transitions are less well-studied and poorly understood, thus providing opportunities for the development of new analysis tools.

VI. SUMMARY

In this perspective, we have provided an overview on the successes and challenges of TDDFT-related approaches for modeling the excited-state properties and processes. A particular emphasis is placed on which electronic structure properties are accessible with which methods, rather than on one single topic like the accuracy of excitation energies.

Firstly, we introduced the main electronic structure quantities required by the description of molecular excited-state

properties and processes, such as the analytic energy derivatives of TDDFT excited state, the NAC and SOC matrix elements, etc. Secondly, we gave a summary of the recent development of hybrid embedding methods for the description of molecular excited states in complex environments, noting that the evaluation of NAC and SOCME accounting for the environment effects, the analytic nuclear derivative of SOCME, and the analytic Hessian of TDDFT/MMpol have not been successfully implemented into the electronic structure packages. Thirdly, we discussed the advantages of three variations of the TDDFT methods. Specifically, TDA might slightly outperform full TDDFT with pure or conventional hybrid functionals; spin-flip DFT is useful for systems with some multireference characters (such as regions around conical interactions); and spin-adiabatic TDDFT could be helpful for studying spin-crossing reactions or the intersystem crossing events. In the end, we elaborated on the challenges in accurately describing interactions between the QM and MM regions, reducing the computational costs associated with modeling excited states in complex environments, and making the results of excited-state calculations physically more transparent and easier to interpret. These challenges have afforded many new opportunities for the development of advanced computational and analysis techniques to treat excited-state-involved processes in complex environments in the future.

ACKNOWLEDGMENTS

WL acknowledges financial support from the National Natural Science Foundation of China (Grant No. 21833006 and 22173074). YS is supported by the National Institutes of Health (grant: R01GM135392), the National Science Foundation (CHE-2102071), and the Office of the Vice President of Research and the College of Art and Sciences at the University of Oklahoma (OU).

DATA AVAILABILITY STATEMENT

The data that support the findings of this study are available within the article.

- ¹T. J. Penfold, E. Gindensperger, C. Daniel, and C. M. Marian, "Spin-vibronic mechanism for intersystem crossing," Chem. Rev. **118**, 6975–7025 (2018).
- ²M. Nottoli, L. Cupellini, F. Lipparini, G. Granucci, and B. Mennucci, "Multiscale Models for Light-Driven Processes," Annu. Rev. Phys. Chem. 72, 489–513 (2021).
- ³B. Mennucci and S. Corni, "Multiscale modelling of photoinduced processes in composite systems," Nat. Rev. Chem. **3**, 315–330 (2019).
- ⁴A. Warshel and M. Levitt, "Theoretical studies of enzymic reactions: Dielectric, electrostatic and steric stabilization of the carbonium ion in the reaction of lysozyme," Journal of Molecular Biology 103, 227–249 (1976).
- ⁵M. J. Field, P. A. Bash, and M. Karplus, "A combined quantum mechanical and molecular mechanical potential for molecular dynamics simulations," Journal of Computational Chemistry 11, 700–733 (1990).
- ⁶J. Tomasi, B. Mennucci, and R. Cammi, "Quantum mechanical continuum solvation models," Chem. Rev. , 2999–3093 (2005).
- ⁷B. Mennucci, "Polarizable continuum model," Wiley Interdiscip. Rev. Comput. Mol. Sci. **2**, 386–404 (2012).

- ⁸C. Cappelli, "Integrated qm/polarizable mm/continuum approaches to-model chiroptical properties of strongly interacting solute–solvent systems," International Journal of Quantum Chemistry 116, 1532–1542 (2016).
- ⁹Y. Gao and D. Neuhauser, "Dynamical quantum-electrodynamics embedding: Combining time-dependent density functional theory and the near-field method," The Journal of Chemical Physics **137**, 074113 (2012), https://doi.org/10.1063/1.4745847.
- ¹⁰H. Chen, J. M. McMahon, M. A. Ratner, and G. C. Schatz, "Classical electrodynamics coupled to quantum mechanics for calculation of molecular optical properties: A RT-TDDFT/FDTD approach," J. Phy. Chem. C 114, 14384–14392 (2010).
- ¹¹C. Yam, L. Meng, G. Chen, Q. Chen, and N. Wong, "Multiscale quantum mechanics/electromagnetics simulation for electronic devices," Phys. Chem. Chem. Phys. 13, 14365–14369 (2011).
- ¹²J. Sun, Z. Ding, Y. Yu, and W. Liang, "Nonlinear features of fano resonance: a qm/em study," Phys. Chem. Chem. Phys. 23, 15994–16004 (2021).
- ¹³ A. V. Akimov and O. V. Prezhdo, "Large-scale computations in chemistry: A bird's eye view of a vibrant field," Chem. Rev. 115, 5797–5890 (2015).
- ¹⁴A. Pribram-Jones, D. A. Gross, and K. Burke, "DFT: A theory full of holes?" Annu. Rev. Phys. Chem. 66, 283–304 (2015).
- ¹⁵N. Mardirossian and M. Head-Gordon, "Thirty years of density functional theory in computational chemistry: an overview and extensive assessment of 200 density functionals," Mol. Phys. 115, 2315–2372 (2017).
- ¹⁶A. Wasserman, J. Nafziger, K. Jiang, M.-C. Kim, E. Sim, and K. Burke, "The importance of being inconsistent," Annu. Rev. Phys. Chem. 68, 555–581 (2017).
- ¹⁷I. H. Hillier, "Chemical reactivity studied by hybrid QM/MM methods," J. Mol. Struct.: THEOCHEM 463, 45–52 (1999).
- ¹⁸C. Sousa, S. Tosoni, and F. Illas, "Theoretical approaches to excited-state-related phenomena in oxide surfaces," Chem. Rev. 113, 4456–4495 (2012).
- ¹⁹H. M. Senn and W. Thiel, "QM/MM methods for biomolecular systems," Angew. Chem. Int. 48, 1198–1229 (2009).
- ²⁰P. Hohenberg and W. Kohn, "Inhomogeneous electron gas," Phys. Rev. 136, B864–B871 (1964).
- ²¹W. Kohn and L. J. Sham, "Self-consistent equations including exchange and correlation effects," Phys. Rev. 140, A1133–A1138 (1965).
- ²²C. Adamo and V. Barone, "A TDDFT study of the electronic spectrum of s-tetrazine in the gas-phase and in aqueous solution," Chem. Phys. Lett. 330, 152–160 (2000).
- ²³C. M. Aikens, S. Li, and G. C. Schatz, "From discrete electronic states to plasmons: TDDFT optical absorption properties of Ag_n(n=10, 20, 35, 56, 84, 120) tetrahedral clusters," J. Phy. Chem. C 112, 11272–11279 (2008).
- ²⁴O. Baseggio, M. D. Vetta, G. Fronzoni, M. Stener, L. Sementa, A. Fortunelli, and A. Calzolari, "Photoabsorption of icosahedral noble metal clusters: An efficient TDDFT approach to large-scale systems," J. Phy. Chem. C 120, 12773–12782 (2016).
- ²⁵D. Grabarek and T. Andruniów, "Assessment of functionals for TDDFT calculations of one- and two-photon absorption properties of neutral and anionic fluorescent proteins chromophores," J. Chem. Theory Comput. 15, 490–508 (2018).
- ²⁶A. Amat, C. Miliani, A. Romani, and S. Fantacci, "DFT/TDDFT investigation on the UV-vis absorption and fluorescence properties of alizarin dye," Phys. Chem. Chem. Phys. 17, 6374–6382 (2015).
- ²⁷B. Wang, X. Wang, W. Wang, and F. Liu, "Exploring the mechanism of fluorescence quenching and aggregation-induced emission of a phenylethylene derivative by QM (CASSCF and TDDFT) and ONIOM (QM:MM) calculations," J. Phy. Chem. C 120, 21850–21857 (2016).
- ²⁸Q. Wan, J. Xia, W. Lu, J. Yang, and C.-M. Che, "Kinetically controlled self-assembly of phosphorescent Au^{III} aggregates and ligand-to-metal-metal charge transfer excited state: A combined spectroscopic and DFT/TDDFT study," J. Am. Chem. Soc. **141**, 11572–11582 (2019).
- ²⁹ M. Babazadeh, P. L. Burn, and D. M. Huang, "Calculating transition dipole moments of phosphorescent emitters for efficient organic light-emitting diodes," Phys. Chem. Chem. Phys. 21, 9740–9746 (2019).
- ³⁰R. Grotjahn and M. Kaupp, "Validation of local hybrid functionals for excited states: Structures, fluorescence, phosphorescence, and vibronic spectra," J. Chem. Theory Comput. 16, 5821–5834 (2020).

- ³¹Y.-Q. Tang and Y.-J. Liu, "Theoretical study on chemiluminescence of H₂O₂-dependent tetrachloro-1,4-benzoquinone," J. Org. Chem. **85**, 9042–9050 (2020).
- ³²B.-W. Ding and Y.-J. Liu, "Bioluminescence of firefly squid via mechanism of single electron-transfer oxygenation and charge-transfer-induced luminescence," J. Am. Chem. Soc. **139**, 1106–1119 (2017).
- ³³C.-G. Min, Q.-B. Liu, Y. Leng, S.-J. Huang, C.-X. Liu, X.-K. Yang, A.-M. Ren, and L. P. da Silva, "Development of firefly oxyluciferin derivatives as pH sensitive fluorescent probes: A DFT/TDDFT study," Comput. Theor. Chem. 1133, 18–24 (2018).
- ³⁴M. Zemmouche, C. García-Iriepa, and I. Navizet, "Light emission colour modulation study of oxyluciferin synthetic analogues via QM and QM/MM approaches," Phys. Chem. Chem. Phys. 22, 82–91 (2020).
- ³⁵M. F. Iozzi, B. Mennucci, J. Tomasi, and R. Cammi, "Excitation energy transfer (EET) between molecules in condensed matter: A novel application of the polarizable continuum model (PCM)," J. Chem. Phys. 120, 7029–7040 (2004).
- ³⁶C. Curutchet, A. Muñoz-Losa, S. Monti, J. Kongsted, G. D. Scholes, and B. Mennucci, "Electronic energy transfer in condensed phase studied by a polarizable QM/MM model," J. Chem. Theory Comput. 5, 1838–1848 (2009).
- ³⁷S. Difley and T. V. Voorhis, "Exciton/charge-transfer electronic couplings in organic semiconductors," J. Chem. Theory Comput. 7, 594–601 (2011).
- ³⁸S. K. Saikin, A. Eisfeld, S. Valleau, and A. Aspuru-Guzik, "Photonics meets excitonics: Natural and artificial molecular aggregates," Nanophotonics 2, 21–38 (2013).
- ³⁹E. Collini, "Spectroscopic signatures of quantum-coherent energy transfer," Chem. Soc. Rev. 42, 4932 (2013).
- ⁴⁰T. Mirkovic, E. E. Ostroumov, J. M. Anna, R. van Grondelle, Govindjee, and G. D. Scholes, "Light absorption and energy transfer in the antenna complexes of photosynthetic organisms," Chem. Rev. 117, 249–293 (2016).
- ⁴¹E. Runge and E. K. U. Gross, "Density-functional theory for time-dependent systems," Phys. Rev. Lett. **52**, 997–1000 (1984).
- ⁴²M. Casida and M. Huix-Rotllant, "Progress in time-dependent density-functional theory," Annu. Rev. Phys. Chem. 63, 287–323 (2012).
- ⁴³B. Jeziorski and H. J. Monkhorst, "Coupled-cluster method for multideterminantal reference states," Phys. Rev. A 24, 1668–1681 (1981).
- ⁴⁴J. D. Watts, J. Gauss, and R. J. Bartlett, "Coupled-cluster methods with noniterative triple excitations for restricted open-shell Hartree–Fock and other general single determinant reference functions. Energies and analytical gradients," J. Chem. Phys. 98, 8718–8733 (1993).
- ⁴⁵J. F. Stanton and R. J. Bartlett, "The equation of motion coupled-cluster method. a systematic biorthogonal approach to molecular excitation energies, transition probabilities, and excited state properties," J. Chem. Phys. 98, 7029–7039 (1993).
- ⁴⁶J. D. Watts and R. J. Bartlett, "Economical triple excitation equationof-motion coupled-cluster methods for excitation energies," Chem. Phys. Lett. 233, 81–87 (1995).
- ⁴⁷S. Hirata, "Higher-order equation-of-motion coupled-cluster methods," J. Chem. Phys. **121**, 51 (2004).
- ⁴⁸ A. I. Krylov, "Equation-of-motion coupled-cluster methods for open-shell and electronically excited species: The hitchhiker's guide to Fock space," Annu. Rev. Phys. Chem. **59**, 433–462 (2008).
- ⁴⁹C. M. Oana and A. I. Krylov, "Cross sections and photoelectron angular distributions in photodetachment from negative ions using equation-of-motion coupled-cluster Dyson orbitals," J. Chem. Phys. **131**, 124114 (2009).
- ⁵⁰R. Klooster, R. Broer, and M. Filatov, "Calculation of X-ray photoelectron spectra with the use of the normalized elimination of the small component method," Chem. Phys. 395, 122–127 (2012).
- ⁵¹I. Josefsson, S. K. Eriksson, N. Ottosson, G. Öhrwall, H. Siegbahn, A. Hagfeldt, H. Rensmo, O. Björneholm, and M. Odelius, "Collective hydrogen-bond dynamics dictates the electronic structure of aqueous I3-," Phys. Chem. Chem. Phys. 15, 20189 (2013).
- ⁵² A. Ponzi, C. Angeli, R. Cimiraglia, S. Coriani, and P. Decleva, "Dynamical photoionization observables of the CS molecule: The role of electron correlation," J. Chem. Phys. **140**, 204304 (2014).
- ⁵³R. J. Magyar and S. Tretiak, "Dependence of spurious charge-transfer excited states on orbital exchange in TDDFT: Large molecules and clusters,"

- J. Chem. Theory Comput. 3, 976-987 (2007).
- ⁵⁴M. Isegawa, R. Peverati, and D. G. Truhlar, "Performance of recent and high-performance approximate density functionals for time-dependent density functional theory calculations of valence and rydberg electronic transition energies," J. Chem. Phys. 137, 244104 (2012).
- ⁵⁵K. Yabana and G. F. Bertsch, "Time-dependent local-density approximation in real time," Phys. Rev. B **54**, 4484 (1996).
- ⁵⁶J. Liu, Z. Guo, J. Sun, and W. Liang, "Theoretical studies on electronic spectroscopy and dynamics with the real-time time-dependent density functional theory," Frontiers of Chemistry in China 5, 11–28 (2010).
- ⁵⁷S. Chen, Y. Kwok, and G. Chen, "Time-dependent density functional theory for open systems and its applications," Acc. Chem. Res. **51**, 383–393 (2018).
- ⁵⁸X. Li, N. Govind, C. Isborn, A. E. DePrince, and K. Lopata, "Real-time time-dependent electronic structure theory," Chem. Rev. **120**, 9951–9993 (2020).
- ⁵⁹T. Nakatsukasa, K. Matsuyanagi, M. Matsuo, and K. Yabana, "Time-dependent density-functional description of nuclear dynamics," Rev. Mod. Phys. 88, 045004 (2016).
- ⁶⁰M. A. L. Marques, A. Castro, G. F. Bertsch, and A. Rubio, "octopus: a first-principles tool for excited electron—ion dynamics," Comput. Phys. Commun. 151, 60–78 (2003).
- ⁶¹M. E. Casida, "Time-dependent density functional response theory for molecules," in *Recent advances in density functional methods* (WORLD SCIENTIFIC, 1995) pp. 155–192.
- ⁶²R. Bauernschmitt and R. Ahlrichs, "Stability analysis for solutions of the closed shell Kohn–Sham equation," J. Chem. Phys. **104**, 9047–9052 (1996).
- ⁶³A. K. Rajagopal, "Time-dependent variational principle and the effective action in density-functional theory and berry's phase," Phys. Rev. A 54, 3916–3922 (1996).
- ⁶⁴A. Görling, "Exact exchange kernel for time-dependent density-functional theory," Int. J. Quantum Chem. **69**, 265–277 (1998).
- ⁶⁵M. E. Casida, C. Jamorski, K. C. Casida, and D. R. Salahub, "Molecular excitation energies to high-lying bound states from time-dependent density-functional response theory: Characterization and correction of the time-dependent local density approximation ionization threshold," J. Chem. Phys. 108, 4439–4449 (1998).
- ⁶⁶B. Champagne, E. A. Perpète, S. J. A. van Gisbergen, E.-J. Baerends, J. G. Snijders, C. Soubra-Ghaoui, K. A. Robins, and B. Kirtman, "Assessment of conventional density functional schemes for computing the polarizabilities and hyperpolarizabilities of conjugated oligomers: An ab initio investigation of polyacetylene chains," J. Chem. Phys. 109, 10489–10498 (1998).
- ⁶⁷C. V. Caillie and R. D. Amos, "Geometric derivatives of excitation energies using SCF and DFT," Chem. Phys. Lett. **308**, 249–255 (1999).
- ⁶⁸F. Furche and R. Ahlrichs, "Adiabatic time-dependent density functional methods for excited state properties," J. Chem. Phys. **117**, 7433–7447 (2002).
- ⁶⁹G. Scalmani, M. J. Frisch, B. Mennucci, J. Tomasi, R. Cammi, and V. Barone, "Geometries and properties of excited states in the gas phase and in solution: Theory and application of a time-dependent density functional theory polarizable continuum model," J. Chem. Phys. **124**, 094107 (2006).
- ⁷⁰J. Liu and W. Liang, "Analytical hessian of electronic excited states in time-dependent density functional theory with Tamm-Dancoff approximation," J. Chem. Phys. 135, 014113 (2011).
- ⁷¹J. Liu and W. Liang, "Analytical approach for the excited-state hessian in time-dependent density functional theory: Formalism, implementation, and performance," J. Chem. Phys. 135, 184111 (2011).
- ⁷²Z. Li and W. Liu, "First-order nonadiabatic coupling matrix elements between excited states: A lagrangian formulation at the CIS, RPA, TD-HF, and TD-DFT levels," J. Chem. Phys. **141**, 014110 (2014).
- ⁷³Z. Li, B. Suo, and W. Liu, "First order nonadiabatic coupling matrix elements between excited states: Implementation and application at the TD-DFT and pp-TDA levels," J. Chem. Phys. 141, 244105 (2014).
- ⁷⁴Q. Ou, G. D. Bellchambers, F. Furche, and J. E. Subotnik, "First-order derivative couplings between excited states from adiabatic TDDFT response theory," J. Chem. Phys. **142**, 064114 (2015).

- ⁷⁵R. Cammi and J. Tomasi, "Nonequilibrium solvation theory for the polarizable continuum model: A new formulation at the SCF level with application to the case of the frequency-dependent linear electric response function," Int. J. Quantum Chem. 56, 465–474 (1995).
- ⁷⁶U. N. Morzan, D. J. A. de Armiño, N. O. Foglia, F. Ramírez, M. C. G. Lebrero, D. A. Scherlis, and D. A. Estrin, "Spectroscopy in complex environments from QM–MM simulations," Chem. Rev. 118, 4071–4113 (2018).
- ⁷⁷L. Yang, S. Nian, G. Zhang, E. Sharman, H. Miao, X. Zhang, X. Chen, Y. Luo, and J. Jiang, "Role of hydrogen bonding in green fluorescent protein-like chromophore emission," Sci. Rep. 9 (2019), 10.1038/s41598-019-47660-0.
- ⁷⁸C. Curutchet and B. Mennucci, "Quantum chemical studies of light harvesting," Chem. Rev. **117**, 294–343 (2016).
- ⁷⁹L. Cupellini, S. Caprasecca, C. A. Guido, F. Müh, T. Renger, and B. Mennucci, "Coupling to charge transfer states is the key to modulate the optical bands for efficient light harvesting in purple bacteria," J. Phys. Chem. Lett. 9, 6892–6899 (2018).
- ⁸⁰D. Loco, S. Protti, B. Mennucci, and A. Mezzetti, "Critical assessment of solvent effects on absorption and fluorescence of 3HF in acetonitrile in the QM/PCM framework: A synergic computational and experimental study," J. Mol. Struct. 1182, 283–291 (2019).
- ⁸¹S. Vukovic, S. Corni, and B. Mennucci, "Fluorescence enhancement of chromophores close to metal nanoparticles. Optimal setup revealed by the polarizable continuum model," J. Phy. Chem. C 113, 121–133 (2008).
- ⁸²R. F. Aroca, "Plasmon enhanced spectroscopy," Phys. Chem. Chem. Phys. 15, 5355 (2013).
- ⁸³S. M. Morton and L. Jensen, "A discrete interaction model/quantum mechanical method to describe the interaction of metal nanoparticles and molecular absorption," J. Chem. Phys. 135, 134103 (2011).
- ⁸⁴Z. Hu and L. Jensen, "A discrete interaction model/quantum mechanical method for simulating plasmon-enhanced two-photon absorption," J. Chem. Theory Comput. 14, 5896–5903 (2018).
- ⁸⁵F. R. Manby, M. Stella, J. D. Goodpaster, and T. F. Miller, "A simple, exact density-functional-theory embedding scheme," J. Chem. Theory Comput. 8, 2564–2568 (2012).
- ⁸⁶S. J. Lee, M. Welborn, F. R. Manby, and T. F. Miller III, "Projection-based wavefunction-in-dft embedding," Acc. Chem. Res. 52, 1359–1368 (2019).
- 87T. A. Wesolowski, S. Shedge, and X. Zhou, "Frozen-density embedding strategy for multilevel simulations of electronic structure," Chem. Rev. 115, 5891–5928 (2015).
- ⁸⁸S. P. Veccham, J. Lee, and M. Head-Gordon, "Making many-body interactions nearly pairwise additive: The polarized many-body expansion approach," J. Chem. Phys. 151, 194101 (2019).
- ⁸⁹H. Nakai and T. Yoshikawa, "Development of an excited-state calculation method for large systems using dynamical polarizability: A divide-andconquer approach at the time-dependent density functional level," J. Chem. Phys. 146, 124123 (2017).
- ⁹⁰J. Tölle, M. Böckers, N. Niemeyer, and J. Neugebauer, "Inter-subsystem charge-transfer excitations in exact subsystem time-dependent density-functional theory," J. Chem. Phys. 151, 174109 (2019).
- ⁹¹J. Tölle and J. Neugebauer, "The seamless connection of local and collective excited states in subsystem time-dependent density functional theory," J. Phys. Chem. Lett. 13, 1003–1018 (2022).
- ⁹²D. Loco, É. Polack, S. Caprasecca, L. Lagardère, F. Lipparini, J.-P. Piquemal, and B. Mennucci, "A QM/MM approach using the AMOEBA polarizable embedding: From ground state energies to electronic excitations," J. Chem. Theory Comput. 12, 3654–3661 (2016).
- ⁹³F. Lipparini, "General linear scaling implementation of polarizable embedding schemes," J. Chem. Theory Comput. 15, 4312–4317 (2019).
- ⁹⁴M. Bondanza, M. Nottoli, L. Cupellini, F. Lipparini, and B. Mennucci, "Polarizable embedding QM/MM: The future gold standard for complex (bio)systems?" Phys. Chem. Chem. Phys. 22, 14433–14448 (2020).
- ⁹⁵F. Plassera, "Theodore: A toolbox for a detailed and automated analysis of electronic excited state computations," J. Chem. Phys. **152**, 084108 (2020).
- ⁹⁶Y. Yuezhi Mao, M. Head-Gordon, and Y. Shao, "Unraveling substituent effects on frontier orbitals of conjugated molecules using an absolutely localized molecular orbital based analysis," Chem. Sci. 137, 8598–8607 (2018).
- ⁹⁷Q. Ge, Y. Mao, and M. Head-Gordon, "Energy decomposition analysis for exciplexes using absolutely localized molecular orbitals," J. Chem. Phys.

- **148**, 064105 (2018).
- ⁹⁸Q. Ge and M. Head-Gordon, "Energy decomposition analysis for excimers using absolutely localized molecular orbitals within time-dependent density functional theory and configuration interaction with single excitations," J. Chem. Theory Comput. 14, 5156–5168 (2018).
- ⁹⁹Y. Orozco-Gonzalez, M. P. Kabir, and S. Gozem, "Electrostatic spectral tuning maps for biological chromophores," J. Phys. Chem. B **123**, 4813– 4824 (2019).
- ¹⁰⁰Z. Pei, Q. Ou, Y. Mao, J. Yang, A. d. Lande, F. Plasser, W. Liang, Z. Shuai, and Y. Shao, "Elucidating the electronic structure of a delayed fluorescence emitter via orbital interactions, excitation energy components, charge-transfer numbers, and vibrational reorganization energies," J. Phys. Chem. Letter 12, 2712–2720 (2021).
- ¹⁰¹M. Head-Gordon, "Quantum chemistry and molecular processes," J. Phys. Chem. **100**, 13213–13225 (1996).
- 102 Y. Yamaguchi, H. F. Schaefer III, Y. Osamura, J. D. Goddard, et al., A new dimension to quantum chemistry: Analytic derivative methods in ab initio molecular electronic structure theory (Oxford University Press, New York, 1904)
- ¹⁰³J. A. Pople, R. Krishnan, H. B. Schlegel, and J. S. Binkley, "Derivative studies in Hartree-Fock and Møller-Plesset theories," Int. J. Quantum Chem. 16, 225–241 (2009).
- ¹⁰⁴R. Cammi, C. Cappelli, S. Corni, and J. Tomasi, "On the calculation of infrared intensities in solution within the polarizable continuum model," J. Phys. Chem. A **104**, 9874–9879 (2000).
- ¹⁰⁵S. Califano, Vibrational States (Wiley, New York, 1976).
- ¹⁰⁶E. B. W. Jr., J. Decius, and P. C. Cross, *Molecular vibrations: The theory of infrared and Raman vibrational spectra* (Dover Publications, New York, 1980).
- ¹⁰⁷N. C. Handy and H. F. Schaefer, "On the evaluation of analytic energy derivatives for correlated wave functions," J. Chem. Phys. 81, 5031–5033 (1984)
- ¹⁰⁸F. Liu, Z. Gan, Y. Shao, C.-P. Hsu, A. Dreuw, M. Head-Gordon, B. T. Miller, B. R. Brooks, J.-G. Yu, T. R. Furlani, and J. Kong, "A parallel implementation of the analytic nuclear gradient for time-dependent density functional theory within the Tamm–Dancoff approximation," Mol. Phys. 108, 2791–2800 (2010).
- ¹⁰⁹F. Furche and R. Ahlrichs, "Erratum: "time-dependent density functional methods for excited state properties" [J. Chem. Phys. 117, 7433 (2002)]," J. Chem. Phys. 121, 12772 (2004).
- ¹¹⁰D. Rappoport and F. Furche, "Analytical time-dependent density functional derivative methods within the RI-J approximation, an approach to excited states of large molecules," J. Chem. Phys. 122, 064105 (2005).
- ¹¹¹D. Si and H. Li, "Analytic energy gradient in combined time-dependent density functional theory and polarizable force field calculation," J. Chem. Phys. 133, 144112 (2010).
- ¹¹²Q. Zeng and W. Liang, "Analytic energy gradient of excited electronic state within TDDFT/MMpol framework: Benchmark tests and parallel implementation," J. Chem. Phys. **143**, 134104 (2015).
- ¹¹³M. F. S. J. Menger, S. Caprasecca, and B. Mennucci, "Excited-state gradients in polarizable QM/MM models: An induced dipole formulation," J. Chem. Theory Comput. 13, 3778–3786 (2017).
- ¹¹⁴Y. Wang and H. Li, "Excited state geometry of photoactive yellow protein chromophore: A combined conductorlike polarizable continuum model and time-dependent density functional study," J. Chem. Phys. 133, 034108 (2010).
- ¹¹⁵C. A. Guido, G. Scalmani, B. Mennucci, and D. Jacquemin, "Excited state gradients for a state-specific continuum solvation approach: The vertical excitation model within a lagrangian TDDFT formulation," J. Chem. Phys. 146, 204106 (2017).
- ¹¹⁶J. Liu and W. Liang, "Analytical second derivatives of excited-state energy within the time-dependent density functional theory coupled with a conductor-like polarizable continuum model," J. Chem. Phys. 138, 024101 (2013).
- ¹¹⁷J. Liu and W. Z. Liang, "Molecular-orbital-free algorithm for the excited-state force in time-dependent density functional theory," J. Chem. Phys. 134, 044114 (2011).
- ¹¹⁸J. Neugebauer, M. Reiher, C. Kind, and B. A. Hess, "Quantum chemical calculation of vibrational spectra of large molecules? Raman and IR spectra for buckminsterfullerene," J. Comput. Chem. 23, 895–910 (2002).

- ¹¹⁹M. Walter and M. Moseler, "Ab initio wavelength-dependent Raman spectra: Placzek approximation and beyond," J. Chem. Theory Comput. 16, 576–586 (2019).
- ¹²⁰D. Porezag and M. R. Pederson, "Infrared intensities and Raman-scattering activities within density-functional theory," Phys. Rev. B **54**, 7830–7836 (1996).
- ¹²¹O. Quinet and B. Champagne, "Time-dependent Hartree-Fock schemes for analytical evaluation of the Raman intensities," J. Chem. Phys. **115**, 6293 (2001).
- ¹²²H.Feshbach, in *Quantum Mechanics* (American Association for the Advancement of Science: Nwe York, 1962).
- ¹²³W. Liang, H. Ma, H. Zang, and C. Ye, "Generalized time-dependent approaches to vibrationally resolved electronic and raman spectra: Theory and applications," International Journal of Quantum Chemistry 115, 550–563 (2015), https://onlinelibrary.wiley.com/doi/pdf/10.1002/qua.24824.
- ¹²⁴F. Duschinsky, "On the interpretation of electronic spectra of polyatomic molecules i: the franck-condon principle," Acta. Phys-Chim. URSS 7, 551 (1937).
- ¹²⁵Q. Ou, Q. Peng, and Z. Shuai, "Toward quantitative prediction of fluorescence quantum efficiency through combining direct vibrational conversion and surface crossing: BODIPYs as example," J. Phys. Chem. Lett. 11, 7790–7797 (2020).
- ¹²⁶W. Domcke and D. R. Yarkony, "Role of conical intersections in molecular spectroscopy and photoinduced chemical dynamics," Annu. Rev. Phys. Chem. 63, 325–352 (2012).
- ¹²⁷J. P. Malhado, M. J. Bearpark, and J. T. Hynes, "Non-adiabatic dynamics close to conical intersections and the surface hopping perspective," Front. Chem. 2 (2014), 10.3389/fchem.2014.00097.
- ¹²⁸M. Hayashi, A. M. Mebel, K. K. Liang, and S. H. Lin, "Ab initio calculations of radiationless transitions between excited and ground singlet electronic states of ethylene," J. Chem. Phys. 108, 2044–2055 (1998).
- ¹²⁹D. J. ROWE, "Equations-of-motion method and the extended shell model," Rev. Mod. Phys. 40, 153–166 (1968).
- ¹³⁰N. Bellonzi, E. Alguire, S. Fatehi, Y. Shao, and J. E. Subotnik, "TD-DFT spin-adiabats with analytic nonadiabatic derivative couplings," J. Chem. Phys. **152**, 044112 (2020).
- ¹³¹S. Matsika, "Electronic structure methods for the description of nonadiabatic effects and conical intersections," Chem. Rev. 121, 9407–9449 (2021).
- ¹³²G. Baryshnikov, B. Minaev, and H. Ågren, "Theory and calculation of the phosphorescence phenomenon," Chem. Rev. 117, 6500–6537 (2017).
- ¹³³C. M. Marian, "Spin-orbit coupling and intersystem crossing in molecules: Spin-orbit coupling," Wiley Interdiscip. Rev. Comput. Mol. Sci. 2, 187–203 (2012).
- ¹³⁴W. Liu and Y. Xiao, "Relativistic time-dependent density functional theories," Chem. Soc. Rev. 47, 4481–4509 (2018).
- ¹³⁵M. Kühn and F. Weigend, "Phosphorescence lifetimes of organic lightemitting diodes from two-component time-dependent density functional theory," J. Chem. Phys. 141, 224302 (2014).
- ¹³⁶S. G. Chiodo and N. Russo, "DFT spin-orbit coupling between singlet and triplet excited states: A case of psoralen compounds," Chem. Phys. Lett. 490, 90–96 (2010).
- ¹³⁷Z. Li, B. Suo, Y. Zhang, Y. Xiao, and W. Liu, "Combining spin-adapted open-shell TD-DFT with spin-orbit coupling," Mol. Phys. 111, 3741–3755 (2013).
- ¹³⁸Q. Ou and J. E. Subotnik, "Electronic relaxation in benzaldehyde evaluated via TD-DFT and localized diabatization: Intersystem crossings, conical intersections, and phosphorescence," J. Phys. Chem. C 117, 19839–19849 (2013).
- ¹³⁹F. Franco de Carvalho, B. F. E. Curchod, T. J. Penfold, and I. Tavernelli, "Derivation of spin-orbit couplings in collinear linear-response TDDFT: A rigorous formulation," J. Chem. Phys. 140, 144103 (2014).
- ¹⁴⁰X. Gao, S. Bai, D. Fazzi, T. Niehaus, M. Barbatti, and W. Thiel, "Evaluation of spin-orbit couplings with linear-response iime-dependent density functional methods," J. Chem. Theory Comput. 13, 515–524 (2017).
- ¹⁴¹F. Dinkelbach, M. Kleinschmidt, and C. M. Marian, "Assessment of interstate spin-orbit couplings from linear response amplitudes," J. Chem. Theory Comput. 13, 749–766 (2017).
- ¹⁴²M. Roemelt, D. Maganas, S. DeBeer, and F. Neese, "A combined DFT and restricted open-shell configuration interaction method including spin-

- orbit coupling: Application to transition metal L-edge X-ray absorption spectroscopy," J. Chem. Phys. 138, 204101 (2013).
- ¹⁴³B. de Souza, G. Farias, F. Neese, and R. Izsák, "Predicting phosphorescence rates of light organic molecules using time-dependent density functional theory and the path integral approach to dynamics," J. Chem. Theory Comput. 15, 1896–1904 (2019).
- ¹⁴⁴J.-X. Duan, Y. Zhou, Z.-Z. Xie, T.-L. Sun, and J. Cao, "Incorporating spin-orbit effects into surface hopping dynamics using the diagonal representation: a linear-response time-dependent density functional theory implementation with applications to 2-thiouracil," Phys. Chem. Chem. Phys. 20, 15445–15454 (2018).
- ¹⁴⁵K. Mori, T. P. M. Goumans, E. van Lenthe, and F. Wang, "Predicting phosphorescent lifetimes and zero-field splitting of organometallic complexes with time-dependent density functional theory including spin-orbit coupling," Phys. Chem. Chem. Phys. 16, 14523–14530 (2014).
- ¹⁴⁶I. Tunell, Z. Rinkevicius, O. Vahtras, P. Sałek, T. Helgaker, and H. Ågren, "Density functional theory of nonlinear triplet response properties with applications to phosphorescence," J. Chem. Phys. 119, 11024–11034 (2003).
- ¹⁴⁷S. Perumal, B. Minaev, and H. Ågren, "Spin-spin and spin-orbit interactions in nanographene fragments: A quantum chemistry approach," J. Chem. Phys. **136**, 104702 (2012).
- ¹⁴⁸A. J. S. Valentine and X. Li, "Toward the evaluation of intersystem crossing rates with variational relativistic methods," J. Chem. Phys. **151**, 084107 (2019).
- ¹⁴⁹S. Lin, Z. Pei, B. Zhang, H. Ma, and W. Liang, "Vibronic coupling effect on the vibrationally resolved electronic spectra and intersystem crossing rates of a tadf emitter: 7-phqad," The Journal of Physical Chemistry A 126, 239–248 (2022), pMID: 34989581, https://doi.org/10.1021/acs.jpca.1c08456.
- ¹⁵⁰M. Chiba, T. Tsuneda, and K. Hirao, "Excited state geometry optimizations by analytical energy gradient of long-range corrected time-dependent density functional theory," J. Chem. Phys. 124, 144106 (2006).
- ¹⁵¹K. A. Nguyen, P. N. Day, and R. Pachter, "Analytical energy gradients of coulomb-attenuated time-dependent density functional methods for excited states," Int. J. Quantum Chem. 110, 2247–2255 (2010).
- ¹⁵²D. W. Silverstein, N. Govind, H. J. J. van Dam, and L. Jensen, "Simulating one-photon absorption and resonance Raman scattering spectra using analytical excited state energy gradients within time-dependent density functional theory," J. Chem. Theory Comput. 9, 5490–5503 (2013).
- ¹⁵³A. M. Burow, J. E. Bates, F. Furche, and H. Eshuis, "Analytical first-order molecular properties and forces within the adiabatic connection random phase approximation," J. Chem. Theory Comput. 10, 180–194 (2013).
- ¹⁵⁴R. Grotjahn, F. Furche, and M. Kaupp, "Development and implementation of excited-state gradients for local hybrid functionals," J. Chem. Theory Comput. 15, 5508–5522 (2019).
- ¹⁵⁵V. Chernyak and S. Mukamel, "Density-matrix representation of nonadia-batic couplings in time-dependent density functional (TDDFT) theories," J. Chem. Phys. 112, 3572–3579 (2000).
- ¹⁵⁶C. Hu, H. Hirai, and O. Sugino, "Nonadiabatic couplings from time-dependent density functional theory: Formulation in the Casida formalism and practical scheme within modified linear response," J. Chem. Phys. 127, 064103 (2007).
- ¹⁵⁷I. Tavernelli, E. Tapavicza, and U. Rothlisberger, "Nonadiabatic coupling vectors within linear response time-dependent density functional theory," J. Chem. Phys. **130**, 124107 (2009).
- ¹⁵⁸R. Send and F. Furche, "First-order nonadiabatic couplings from time-dependent hybrid density functional response theory: Consistent formalism, implementation, and performance," J. Chem. Phys. **132**, 044107 (2010).
- ¹⁵⁹I. Tavernelli, B. F. E. Curchod, A. Laktionov, and U. Rothlisberger, "Nona-diabatic coupling vectors for excited states within time-dependent density functional theory in the Tamm–Dancoff approximation and beyond," J. Chem. Phys. 133, 194104 (2010).
- ¹⁶⁰Y. Shao, M. Head-Gordon, and A. I. Krylov, "The spin-flip approach within time-dependent density functional theory: Theory and applications to diradicals," J. Chem. Phys. 118, 4807–4818 (2003).
- ¹⁶¹F. Wang and T. Ziegler, "Time-dependent density functional theory based on a noncollinear formulation of the exchange-correlation potential," J. Chem. Phys. 121, 12191 (2004).

- ¹⁶²Y. A. Bernard, Y. Shao, and A. I. Krylov, "General formulation of spin-flip time-dependent density functional theory using non-collinear kernels: Theory, implementation, and benchmarks," J. Chem. Phys. 136, 204103 (2012).
- ¹⁶³X. Zhang and J. M. Herbert, "Spin-flip, tensor equation-of-motion configuration interaction with a density-functional correction: A spin-complete method for exploring excited-state potential energy surfaces," J. Chem. Phys. 143, 234107 (2015).
- ¹⁶⁴M. Seth, G. Mazur, and T. Ziegler, "Time-dependent density functional theory gradients in the amsterdam density functional package: geometry optimizations of spin-flip excitations," Theor. Chem. Acc. 129, 331–342 (2010).
- ¹⁶⁵S. Lee, E. E. Kim, H. Nakata, S. Lee, and C. H. Choi, "Efficient implementations of analytic energy gradient for mixed-reference spin-flip time-dependent density functional theory (MRSF-TDDFT)," J. Chem. Phys. 150, 184111 (2019).
- ¹⁶⁶X. Zhang and J. M. Herbert, "Analytic derivative couplings for spin-flip configuration interaction singles and spin-flip time-dependent density functional theory," J. Chem. Phys. 141, 064104 (2014).
- ¹⁶⁷X. Zhang and J. M. Herbert, "Analytic derivative couplings in time-dependent density functional theory: Quadratic response theory versus pseudo-wavefunction approach," J. Chem. Phys. 142, 064109 (2015).
- ¹⁶⁸N. Bellonzi, G. R. Medders, E. Epifanovsky, and J. E. Subotnik, "Configuration interaction singles with spin-orbit coupling: Constructing spin-adiabatic states and their analytical nuclear gradients," J. Chem. Phys. 150, 014106 (2019).
- ¹⁶⁹N. Minezawa and T. Nakajima, "Trajectory surface hopping molecular dynamics simulation by spin-flip time-dependent density functional theory," J. Chem. Phys. **150**, 204120 (2019).
- ¹⁷⁰R. Cammi and B. Mennucci, "Linear response theory for the polarizable continuum model," J. Chem. Phys. 110, 9877–9886 (1999).
- ¹⁷¹R. Improta, V. Barone, G. Scalmani, and M. J. Frisch, "A state-specific polarizable continuum model time dependent density functional theory method for excited state calculations in solution," J. Chem. Phys. 125, 054103 (2006).
- ¹⁷²Z.-Q. You, J.-M. Mewes, A. Dreuw, and J. M. Herbert, "Comparison of the marcus and pekar partitions in the context of non-equilibrium, polarizablecontinuum solvation models," J. Chem. Phys. 143, 204104 (2015).
- ¹⁷³T.-J. Bi, L.-K. Xu, F. Wang, and X.-Y. Li, "Solvent effects for vertical absorption and emission processes in solution using a self-consistent state specific method based on constrained equilibrium thermodynamics," Phys. Chem. Chem. Phys. 20, 13178–13190 (2018).
- ¹⁷⁴C. A. Guido, M. Rosa, R. Cammi, and S. Corni, "An open quantum system theory for polarizable continuum models," J. Chem. Phys. **152**, 174114 (2020).
- ¹⁷⁵Q. Zeng, J. Liu, and W. Liang, "Molecular properties of excited electronic state: Formalism, implementation, and applications of analytical second energy derivatives within the framework of the time-dependent density functional theory/molecular mechanics," J. Chem. Phys. **140**, 18A506 (2014).
- ¹⁷⁶M. Wohlgemuth, V. Bonačić-Koutecký, and R. Mitrić, "Time-dependent density functional theory excited state nonadiabatic dynamics combined with quantum mechanical/molecular mechanical approach: Photodynamics of indole in water," J. Chem. Phys. 135, 054105 (2011).
- ¹⁷⁷N. Minezawa and T. Nakajima, "Quantum mechanical/molecular mechanical trajectory surface hopping molecular dynamics simulation by spin-flip time-dependent density functional theory," J. Chem. Phys. **152**, 024119 (2020).
- ¹⁷⁸S. M. Morton and L. Jensen, "A discrete interaction model/quantum mechanical method for describing response properties of molecules adsorbed on metal nanoparticles," J. Chem. Phys. 133, 074103 (2010).
- ¹⁷⁹D. Kosenkov and L. V. Slipchenko, "Solvent effects on the electronic transitions ofp-nitroaniline: A QM/EFP study," J. Phy. Chem. A 115, 392–401 (2011).
- ¹⁸⁰N. Minezawa and M. S. Gordon, "Optimizing conical intersections of solvated molecules: The combined spin-flip density functional theory/effective fragment potential method," J. Chem. Phys. **137**, 034116 (2012).
- ¹⁸¹T. Giovannini, R. R. Riso, M. Ambrosetti, A. Puglisi, and C. Cappelli, "Electronic transitions for a fully polarizable QM/MM approach based on

- fluctuating charges and fluctuating dipoles: Linear and corrected linear response regimes," J. Chem. Phys. **151**, 174104 (2019).
- ¹⁸²N. Minezawa, N. D. Silva, F. Zahariev, , and M. S. Gordon, "Implementation of the analytic energy gradient for the combined time-dependent density functional theory/effective fragment potential method: Application to excited-state molecular dynamics simulations," J. Chem. Phys. 134, 054111 (2011).
- ¹⁸³J. M. P. Martirez and E. A. Carter, "Excited-state N₂ dissociation pathway on Fe-functionalized Au," J. Am. Chem. Soc. **139**, 4390–4398 (2017).
- ¹⁸⁴J. M. P. Martirez and E. A. Carter, "Prediction of a low-temperature N₂ dissociation catalyst exploiting near-IR-to-visible light nanoplasmonics," Sci. Adv. 3, eaao4710 (2017).
- ¹⁸⁵S. Mukherjee, F. Libisch, N. Large, O. Neumann, L. V. Brown, J. Cheng, J. B. Lassiter, E. A. Carter, P. Nordlander, and N. J. Halas, "Hot electrons do the impossible: Plasmon-induced dissociation of H₂ on Au," Nano Lett. 13, 240–247 (2013).
- ¹⁸⁶G. Mie, "Beiträge zur optik trüber medien, speziell kolloidaler metallösungen," Ann. Phys. 330, 377–445 (1908).
- ¹⁸⁷S. Corni and J. Tomasi, "Enhanced response properties of a chromophore physisorbed on a metal particle," J. Chem. Phys. **114**, 3739 (2001).
- ¹⁸⁸B. T. Draine and P. J. Flatau, "Discrete-dipole approximation for scattering calculations," J. Opt. Soc. Am. A 11, 1491 (1994).
- ¹⁸⁹W. H. Yang, G. C. Schatz, and R. P. Van Duyne, "Discrete dipole approximation for calculating extinction and Raman intensities for small particles with arbitrary shapes," J. Chem. Phys. 103, 869 (1995).
- ¹⁹⁰F. J. García de Abajo and A. Howie, "Relativistic electron energy loss and electron-induced photon emission in inhomogeneous dielectrics," Phys. Rev. Lett. **80**, 869 (1995).
- ¹⁹¹ F. Hao, C. L. Nehl, J. H. Hafner, and P. Nordlander, "Plasmon resonances of a gold nanostar," Nano Lett. 7, 729–732 (2007).
- ¹⁹²S. Kmiecik, D. Gront, M. Kolinski, L. Wieteska, A. E. Dawid, and A. Kolinski, "Coarse-grained protein models and their applications," Chem. Rev. 116, 7898–7936 (2016).
- ¹⁹³X. Chen, J. E. Moore, M. Zekarias, and L. Jensen, "Atomistic electrodynamics simulations of bare and ligand-coated nanoparticles in the quantum size regime," Nat. Commun. 6, 8921 (2015).
- ¹⁹⁴J. Lim, S. Kang, J. Kim, W. Y. Kim, and S. Ryu, "Non-empirical atomistic dipole-interaction-model for quantum plasmon simulation of nanoparticles," Scientific Reports 7, 15775 (2017).
- ¹⁹⁵L. L. Jensen and L. Jensen, "Electrostatic interaction model for the calculation of the polarizability of large noble metal nanoclusters," J. Phys. Chem. C 112, 15697–15703 (2008).
- ¹⁹⁶V. I. Zakomirnyi, Z. Rinkevicius, G. V. Baryshnikov, L. K. Sørensen, and H. Ågren, "Extended discrete interaction model: Plasmonic excitations of Silver nanoparticles," J. Phys. Chem. C 123, 28867–28880 (2019).
- ¹⁹⁷J. Applequist, "An atom dipole interaction model for molecular optical properties," Acc. Chem. Res. 10, 79–85 (1977).
- ¹⁹⁸L. Jensen, P.-O. Åstrand, A. Osted, J. Kongsted, and K. V. Mikkelsen, "Polarizability of molecular clusters as calculated by a dipole interaction model," J. Chem. Phys. 116, 4001 (2002).
- ¹⁹⁹H. S. Smalo, P.-O. Åstrand, and A. Mayer, "Combined nonmetallic electronegativity equalisation and point-dipole interaction model for the frequency-dependent polarisability," Mol. Phys. 111, 1470–1481 (2013).
- ²⁰⁰N. Davari, S. Haghdani, P.-O. Åstrand, and G. C. Schatz, "Local electric field factors by a combined charge-transfer and point-dipole interaction model," RSC Adv. 5, 31594–31605 (2015).
- ²⁰¹A. Mayer, "Formulation in terms of normalized propagators of a charge-dipole model enabling the calculation of the polarization properties of fullerenes and carbon nanotubes," Phys. Rev. B 75, 045407 (2007).
- ²⁰²A. Mayer, A. L. González, C. M. Aikens, and G. C. Schatz, "A charge–dipole interaction model for the frequency-dependent polarizability of silver clusters," Nanotechnology 20, 195204 (2009).
- ²⁰³T. Vreven and K. Morokuma, "Chapter 3 hybrid methods: Oniom(qm:mm) and qm/mm," Annual Reports in Computational Chemistry, 2, 35–51 (2006).
- ²⁰⁴H. Lin and D. G. Truhlar, "QM/MM: what have we learned, where are we, and where do we go from here?" Theor. Chem. Acc. 117, 185–199 (2006).
- ²⁰⁵Y. Shao, Y. Mei, D. Sundholm, and V. R. I. Kaila, "Benchmarking the performance of time-dependent density functional theory methods on biochromophores," J. Chem. Theory Comput. 16, 587–600 (2019).

- ²⁰⁶A. D. McLACHLAN and M. A. BALL, "Time-dependent hartree—fock theory for molecules," Rev. Mod. Phys. 36, 844–855 (1964).
- ²⁰⁷C. Hu, O. Sugino, and K. Watanabe, "Performance of tamm-dancoff approximation on nonadiabatic couplings by time-dependent density functional theory," The Journal of Chemical Physics **140**, 054106 (2014), https://doi.org/10.1063/1.4862904.
- ²⁰⁸O. Christiansen, H. Koch, and P. Jørgensen, "The second-order approximate coupled cluster singles and doubles model cc2," Chem. Phys. Lett. 243, 409–418 (1995).
- ²⁰⁹F. Weigend and R. Ahlrichs, "Balanced basis sets of split valence, triple zeta valence and quadruple zeta valence quality for h to rn: Design and assessment of accuracy," Phys. Chem. Chem. Phys. 7, 3297–3305 (2005).
- ²¹⁰Z. Li and W. Liu, "Spin-adapted open-shell random phase approximation and time-dependent density functional theory. I. Theory," J. Chem. Phys. 133, 064106 (2010).
- ²¹¹Z. Li, W. Liu, Y. Zhang, and B. Suo, "Spin-adapted open-shell time-dependent density functional theory. II. Theory and pilot application," J. Chem. Phys. **134**, 134101 (2011).
- ²¹²B. G. Levine, C. Ko, J. Quenneville, and T. J. Martínez, "Conical intersections and double excitations in time-dependent density functional theory," Mol. Phys. **104**, 1039–1051 (2006).
- ²¹³J. C. Tully, "Molecular dynamics with electronic transitions," J. Chem. Phys. **93**, 1061–1071 (1990).
- ²¹⁴Y. Tao, Z. Pei, N. Bellonzi, Y. Mao, Z. Zou, W. Liang, Z. Yang, and Y. Shao, "Constructing spin-adiabatic states for the modeling of spincrossing reactions. I. A shared-orbital implementation," Int. J. Quantum Chem. 120, e26123 (2020).
- ²¹⁵J. L. Payton, S. M. Morton, J. E. Moore, and L. Jensen, "A discrete interaction model/quantum mechanical method for simulating surface-enhanced Raman spectroscopy," J. Chem. Phys. 136, 214103 (2012).
- ²¹⁶Z. Pei, Y. Mao, Y. Shao, and W. Z. Liang, "Analytic high-order energy derivatives for metal nanoparticle-mediated infrared and raman scattering spectra within the framework of quantum mechanics/molecular mechanics model with induced charges and dipoles," ChemRxiv (2022), 10.26434/chemrxiv-2022-dwdp4.
- ²¹⁷E. Epifanovsky, A. T. B. Gilbert, X. Feng, J. Lee, Y. Mao, N. Mardirossian, P. Pokhilko, A. F. White, M. P. Coons, A. L. Dempwolff, Z. Gan, D. Hait, P. R. Horn, L. D. Jacobson, I. Kaliman, J. Kussmann, A. W. Lange, K. U. Lao, D. S. Levine, J. Liu, S. C. McKenzie, A. F. Morrison, K. D. Nanda, F. Plasser, D. R. Rehn, M. L. Vidal, Z.-Q. You, Y. Zhu, B. Alam, B. J. Albrecht, A. Aldossary, E. Alguire, J. H. Andersen, V. Athavale, D. Barton, K. Begam, A. Behn, N. Bellonzi, Y. A. Bernard, E. J. Berquist, H. G. A. Burton, A. Carreras, K. Carter-Fenk, R. Chakraborty, A. D. Chien, K. D. Closser, V. Cofer-Shabica, S. Dasgupta, M. de Wergifosse, J. Deng, M. Diedenhofen, H. Do, S. Ehlert, P.-T. Fang, S. Fatehi, Q. Feng, T. Friedhoff, J. Gayvert, Q. Ge, G. Gidofalvi, M. Goldey, J. Gomes, C. E. González-Espinoza, S. Gulania, A. O. Gunina, M. W. D. Hanson-Heine, P. H. P. Harbach, A. Hauser, M. F. Herbst, M. Hernández Vera, M. Hodecker, Z. C. Holden, S. Houck, X. Huang, K. Hui, B. C. Huynh, M. Ivanov, Á. Jász, H. Ji, H. Jiang, B. Kaduk, S. Köhler, K. Khistyaev, J. Kim, G. Kis, P. Klunzinger, Z. Koczor-Benda, J. H. Koh, D. Kosenkov, L. Koulias, T. Kowalczyk, C. M. Krauter, K. Kue, A. Kunitsa, T. Kus, I. Ladjánszki, A. Landau, K. V. Lawler, D. Lefrancois, S. Lehtola, R. R. Li, Y.-P. Li, J. Liang, M. Liebenthal, H.-H. Lin, Y.-S. Lin, F. Liu, K.-Y. Liu, M. Loipersberger, A. Luenser, A. Manjanath, P. Manohar, E. Mansoor, S. F. Manzer, S.-P. Mao, A. V. Marenich, T. Markovich, S. Mason, S. A. Maurer, P. F. McLaughlin, M. F. S. J. Menger, J.-M. Mewes, S. A. Mewes, P. Morgante, J. W. Mullinax, K. J. Oosterbaan, G. Paran, A. C. Paul, S. K. Paul, F. Pavošević, Z. Pei, S. Prager, E. I. Proynov, Á. Rák, E. Ramos-Cordoba, B. Rana, A. E. Rask, A. Rettig, R. M. Richard, F. Rob, E. Rossomme, T. Scheele, M. Scheurer, M. Schneider, N. Sergueev, S. M. Sharada, W. Skomorowski, D. W. Small, C. J. Stein, Y.-C. Su, E. J. Sundstrom, Z. Tao, J. Thirman, G. J. Tornai, T. Tsuchimochi, N. M. Tubman, S. P. Veccham, O. Vydrov, J. Wenzel, J. Witte, A. Yamada, K. Yao, S. Yeganeh, S. R. Yost, A. Zech, I. Y. Zhang, X. Zhang, Y. Zhang, D. Zuev, A. Aspuru-Guzik, A. T. Bell, N. A. Besley, K. B. Bravaya, B. R. Brooks, D. Casanova, J.-D. Chai, S. Coriani, C. J. Cramer, G. Cserey, A. E. DePrince, R. A. DiStasio, A. Dreuw, B. D. Dunietz, T. R. Furlani, W. A. Goddard, S. Hammes-Schiffer, T. Head-Gordon, W. J. Hehre, C.-P. Hsu, T.-C. Jagau, Y. Jung, A. Klamt, J. Kong, D. S. Lambrecht, W. Liang,

- N. J. Mayhall, C. W. McCurdy, J. B. Neaton, C. Ochsenfeld, J. A. Parkhill, R. Peverati, V. A. Rassolov, Y. Shao, L. V. Slipchenko, T. Stauch, R. P. Steele, J. E. Subotnik, A. J. W. Thom, A. Tkatchenko, D. G. Truhlar, T. Van Voorhis, T. A. Wesolowski, K. B. Whaley, H. L. Woodcock, P. M. Zimmerman, S. Faraji, P. M. W. Gill, M. Head-Gordon, J. M. Herbert, and A. I. Krylov, "Software for the frontiers of quantum chemistry: An overview of developments in the Q-Chem 5 package," J. Chem. Phys. 155, 084801 (2021).
- ²¹⁸R. Z. Khaliullin, E. A. Cobar, R. C. Lochan, A. T. Bell, and M. Head-Gordon, "Unravelling the origin of intermolecular interactions using absolutely localized molecular orbitals," J. Phys. Chem. A 111, 8753–8765 (2007).
- ²¹⁹B. H. Besler, K. M. Merz Jr, and P. A. Kollman, "Atomic charges derived from semiempirical methods," J. Comput. Chem. 11, 431–439 (1990).
- ²²⁰C. M. Breneman and K. B. Wiberg, "Determining atom-centered monopoles from molecular electrostatic potentials. the need for high sampling density in formamide conformational analysis," J. Comput. Chem. 11, 361–373 (1990).
- ²²¹J. Rezac and A. de la Lande, J. Chem. Theory Comput. 11, 528–537 (2015).
- ²²²J.-D. Chai and M. Head-Gordon, "Long-range corrected hybrid density functionals with damped atom-atom dispersion corrections," Phys. Chem. Chem. Phys. 10, 6615–6620 (2008).
- ²²³ A. Kovyrshin and J. Neugebauer, "State-selective optimization of local excited electronic states in extended systems," J. Chem. Phys. **133**, 174114 (2010).
- ²²⁴A. Kovyrshin and J. Neugebauer, "Potential-energy surfaces of local excited states from subsystem- and selective Kohn–Sham-TDDFT," Chem. Phys. 391, 147–156 (2011).
- ²²⁵A. Kovyrshin, F. D. Angelis, and J. Neugebauer, "Selective TDDFT with automatic removal of ghost transitions: application to a perylene-dyesensitized solar cell model," Phys. Chem. Chem. Phys. 14, 8608 (2012).
- ²²⁶R. Z. Khaliullin, M. Head-Gordon, and A. T. Bell, "An efficient self-consistent field method for large systems of weakly interacting components," J. Chem. Phys. **124**, 204105 (2006).
- ²²⁷K. D. Closser, Q. Ge, Y. Mao, Y. Shao, and M. Head-Gordon, "Superposition of fragment excitations for excited states of large clusters with application to helium clusters," J. Chem. Theory Comput. 11, 5791–5803 (2015).
- ²²⁸E. R. Kuechler, T. J. Giese, and D. M. York, "Charge-dependent many-body exchange and dispersion interactions in combined QM/MM simulations," J. Chem. Phys. **143**, 234111 (2015).
- ²²⁹T. Giovannini, P. Lafiosca, and C. Cappelli, "A general route to include pauli repulsion and quantum dispersion effects in QM/MM approaches," J. Chem. Theory Comput. 13, 4854–4870 (2017).
- ²³⁰C. Curutchet, L. Cupellini, J. Kongsted, S. Corni, L. Frediani, A. H. Steindal, C. A. Guido, G. Scalmani, and B. Mennucci, "Density-dependent formulation of dispersion–repulsion interactions in hybrid multiscale quantum/molecular mechanics (QM/MM) models," J. Chem. Theory Comput. 14, 1671–1681 (2018).
- ²³¹ A. Tkatchenko and M. Scheffler, "Accurate molecular van der Waals interactions from ground-state electron density and free-atom reference data," Phys. Rev. Lett. **102**, 073005 (2009).
- ²³²L. V. Slipchenko, M. S. Gordon, and K. Ruedenberg, "Dispersion interactions in QM/EFP," J. Phy. Chem. A 121, 9495–9507 (2017).
- ²³³C. I. V. Rojas, J. Fine, and L. V. Slipchenko, "Exchange-repulsion energy in QM/EFP," J. Chem. Phys. **149**, 094103 (2018).
- ²³⁴C. I. V. Rojas and L. V. Slipchenko, "Exchange repulsion in quantum mechanical/effective fragment potential excitation energies: Beyond polarizable embedding," J. Chem. Theory Comput. 16, 6408–6417 (2020).
- ²³⁵S. Grimme, "A simplified Tamm-Dancoff density functional approach for the electronic excitation spectra of very large molecules," J. Chem. Phys. 138, 244104 (2013).
- ²³⁶C. Bannwarth and S. Grimme, "A simplified time-dependent density functional theory approach for electronic ultraviolet and circular dichroism spectra of very large molecules," Comput. Theor. Chem. **1040-1041**, 45–53 (2014).
- 237T. Risthaus, A. Hansen, and S. Grimme, "Excited states using the simplified Tamm-Dancoff-approach for range-separated hybrid density functionals: development and application," Phys. Chem. Chem. Phys. 16,

- 14408-14419 (2014).
- ²³⁸P. Pulay and G. Fogarasi, "Fock matrix dynamics," Chem. Phys. Lett. 386, 272–278 (2004).
- ²³⁹J. M. Herbert and M. Head-Gordon, "Accelerated, energy-conserving Born-Oppenheimer molecular dynamics via Fock matrix extrapolation," Phys. Chem. Chem. Phys. 7, 3269 (2005).
- ²⁴⁰ A. M. N. Niklasson, "Extended Born-Oppenheimer molecular dynamics," Phys. Rev. Lett. **100**, 123004 (2008).
- ²⁴¹A. M. N. Niklasson, "Density-matrix based extended lagrangian Born-Oppenheimer molecular dynamics," J. Chem. Theory Comput. 16, 3628–3640 (2020)
- ²⁴²R. P. Steele and J. C. Tully, "Accelerated ab initio molecular dynamics with response equation extrapolation," Chem. Phys. Lett. **500**, 167 (2010).
- ²⁴³F. Segatta, L. Cupellini, M. Garavelli, and B. Mennucci, "Quantum chemical modeling of the photoinduced activity of multichromophoric biosystems," Chem. Rev. 119, 9361–9380 (2019).
- ²⁴⁴E. Brunk and U. Rothlisberger, "Mixed quantum mechanical/molecular mechanical molecular dynamics simulations of biological systems in ground and electronically excited states," Chem. Rev. 115, 6217–6263 (2015).
- ²⁴⁵P. Ren and J. W. Ponder, "Polarizable atomic multipole water model for molecular mechanics simulation," J. Phy. Chem. B **107**, 5933–5947 (2003).
- ²⁴⁶P. Pulay, "Convergence acceleration of iterative sequences. the case of scf iteration," Chem. Phys. Lett. **73**, 393–398 (1980).
- ²⁴⁷P. Pulay, "Improved SCF convergence acceleration," J. Comput. Chem. 3, 556–560 (1982).
- ²⁴⁸W. Wang and R. D. Skeel, "Fast evaluation of polarizable forces," J. Chem. Phys. 123, 164107 (2005).
- ²⁴⁹A. C. Simmonett, F. C. Pickard, Y. Shao, T. E. Cheatham, and B. R. Brooks, "Efficient treatment of induced dipoles," J. Chem. Phys. 143, 074115 (2015).
- ²⁵⁰F. Aviat, A. Levitt, B. Stamm, Y. Maday, P. Ren, J. W. Ponder, L. Lagardère, and J.-P. Piquemal, "Truncated conjugate gradient: An optimal strategy for the analytical evaluation of the many-body polarization energy and forces in molecular simulations," J. Chem. Theory Comput. 13, 180–190 (2016).
- 251 F. Aviat, L. Lagardère, and J.-P. Piquemal, "The truncated conjugate gradient (TCG), a non-iterative/fixed-cost strategy for computing polarization in

- molecular dynamics: Fast evaluation of analytical forces," J. Chem. Phys. **147**, 161724 (2017).
- ²⁵²D. Nocito and G. J. O. Beran, "Fast divide-and-conquer algorithm for evaluating polarization in classical force fields," J. Chem. Phys. **146**, 114103 (2017).
- ²⁵³D. Nocito and G. J. O. Beran, "Massively parallel implementation of divide-and-conquer jacobi iterations using particle-mesh ewald for force field polarization," J. Chem. Theory Comput. 14, 3633–3642 (2018).
- ²⁵⁴D. Nocito and G. J. O. Beran, "Reduced computational cost of polarizable force fields by a modification of the always stable predictor-corrector," J. Chem. Phys. **150**, 151103 (2019).
- ²⁵⁵O. Demerdash and T. Head-Gordon, "Convergence of the many-body expansion for energy and forces for classical polarizable models in the condensed phase," J. Chem. Theory Comput. 12, 3884–3893 (2016).
- ²⁵⁶A. Albaugh, O. Demerdash, and T. Head-Gordon, "An efficient and stable hybrid extended lagrangian/self-consistent field scheme for solving classical mutual induction," J. Chem. Phys. 143, 174104 (2015).
- ²⁵⁷A. Albaugh, A. M. N. Niklasson, and T. Head-Gordon, "Accurate classical polarization solution with no self-consistent field iterations," J. Phys. Chem. Lett. 8, 1714–1723 (2017).
- ²⁵⁸A. Albaugh, T. Head-Gordon, and A. M. N. Niklasson, "Higher-order extended lagrangian Born-Oppenheimer molecular dynamics for classical polarizable models," J. Chem. Theory Comput. 14, 499–511 (2018).
- ²⁵⁹M. J. G. Peach, P. Benfield, T. Helgaker, and D. J. Tozer, "Excitation energies in density functional theory: An evaluation and a diagnostic test," J. Chem. Phys. **128**, 044118 (2008).
- ²⁶⁰F. Plasser, M. Wormit, and A. Dreuw, "New tools for the systematic analysis and visualization of electronic excitations. i. formalism," J. Chem. Phys. 141, 024106 (2014).
- ²⁶¹F. Plasser, S. A. Bäppler, M. Wormit, and A. Dreuw, "New tools for the systematic analysis and visualization of electronic excitations. II. applications," J. Chem. Phys. **141**, 024107 (2014).
- ²⁶²Z. Pei, J. Yang, J. Deng, Y. Mao, Q. Wu, Z. Yang, B. Wang, C. M. Aikens, W. Liang, and Y. Shao, "Analysis and visualization of energy densities. II. insights from linear-response time-dependent density functional theory calculations," Phys. Chem. Chem. Phys. 22, 26852–26864 (2020).